

Supplementary Materials for

Edge Functionalization of Bulk γ -Graphyne Facilitates Mechanical Exfoliation and Modulates the Mode of Sheet Stacking

Claire M.B. Bolding,^a Tejaswini K. Haraniya,^a Grace L. Parker,^a William B. Martin,^a Victor G. Desyatkin,^a Logan Heck,^a Konstantin Bukhryakov,^b and Valentin O. Rodionov^{a*}

^a Department of Macromolecular Science and Engineering, Case Western Reserve University; 2100 Adelbert Road, Cleveland, OH 44106 USA

^b Department of Chemistry and Biochemistry, Florida International University; 11200 SW 8th Street, Miami, FL, 33199 USA

*Correspondence to: Prof. Valentin O. Rodionov. Email: vor2@case.edu

Table of Contents

1. Nomenclature and Abbreviations	3
2. Materials and Methods.....	4
Materials	4
Synthetic Methods	4
NMR Spectrometry.....	4
Gas Chromatography and Mass Spectrometry	4
Infrared Spectroscopy	4
Melting Points.....	5
Transmission Electron Microscopy	5
Atomic Force Microscopy	5
X-ray Photoelectron Spectroscopy	5
Thermogravimetric Analysis	5
Differential Scanning Calorimetry.....	6
UV-Vis Spectroscopy	6
SAED Simulation.....	6
3. Synthesis of small molecules	7
1,3,5-tribromo-2,4,6-triiodobenzene.....	7
((2,4,6-tribromobenzene-1,3,5-triyl)tris(ethyne-2,1-diyl))tris(trimethylsilane)	7
TBTEB.....	8
Methyl 2-phenylhydrazine-1-carbodithioate	8
<i>N,N</i> -Diethylphenylazothioformamide.....	9
4. Synthesis of Carbon Materials	10
General Synthetic Procedure for γ -Graphyne (GY-Br)	10
Edge Functionalization of GY-Br in One Pot by Sonogashira Coupling.....	10
Edge Functionalization of GY-Br by CuAAC Click Chemistry	10
5. Characterization	11
¹ H NMR	11
¹³ C NMR.....	16
Mass Spectrometry.....	21
XPS	26
TGA	37
TEM and SAED.....	38
UV/Visible Spectroscopy of Dispersions	42
6. References.....	43

1. Nomenclature and Abbreviations

Table S1. Nomenclature and Abbreviations

Abbreviation	Description
AFM	Atomic Force Microscopy
ATR	Attenuated Total Reflectance
DCM	Dichloromethane
DLS	Dynamic Light Scattering
DMSO	Dimethylsulfoxide
DSC	Differential Scanning Calorimetry
EDS	Energy Dispersive X-ray Spectroscopy
ETD	Everhart-Thornley Detector
EI-MS	Electron Ionization Mass Spectrometry
FTIR	Fourier Transform Infrared Spectroscopy
GC-MS	Gas Chromatography – Mass Spectrometry
MSD	Mass Selective Detector
ppm	parts per million
Py	Pyridine
SAED	Selected Area Electron Diffraction
SEM	Scanning Electron Microscopy
TBAF	Tetra-n-Butylammonium Fluoride
TBTEB	1,3,5-Tribromo-2,4,6-triethynylbenzene
TEA	Triethylamine
TEM	Transmission Electron Microscopy
TGA	Thermogravimetric Analysis
THF	Tetrahydrofuran
TLC	Thin-Layer Chromatography
TSP	Thermal Separation Probe
UV-Vis	Ultraviolet-Visible

2. Materials and Methods

Materials

All reagents and solvents were acquired from commercial suppliers (Acros Organics, Sigma-Aldrich, TCI Chemicals, Fisher Scientific, VWR International, and Strem) and used without further purification, unless otherwise noted. THF was distilled over Na/benzophenone. Triethylamine was distilled over CaH₂. Anhydrous pyridine was purchased from Acros in AcroSeal packaging and used without further purification.

Synthetic Methods

Reactions were monitored by thin-layer chromatography carried out on 0.25 mm MilliporeSigma aluminum-backed silica gel plates (60F-254). Plates were visualized using 254 nm UV light and basic potassium permanganate stain (1.5 g KMnO₄, 0.5 g NaOH, and 10 g K₂CO₃ in 150 ml water; terminal alkynes stain yellow). Flash chromatography was performed on Luknova SuperSepTM (230-400 mesh) silica gel. Reactions requiring anhydrous or air-free conditions were performed under positive pressure of Ar using standard Schlenk line techniques.

NMR Spectrometry

Routine NMR spectra were recorded on a Bruker Avance III HD 500 spectrometer operating at 500.24 (¹H), 125.79 (¹³C) MHz and equipped with Bruker Ascend 500 MHz US Narrow Bore Magnet and Broadband Prodigy TCI CryoProbe. NMR spectra were referenced to TMS (¹H, ¹³C) or residual solvent peaks. Chemical shifts (δ) are reported in parts per million (ppm).

Gas Chromatography and Mass Spectrometry

GC-MS and EI-MS analyses were performed on an Agilent 7890B/5977B GC/MSD instrument equipped with an Agilent 7890B automatic liquid sampler, Agilent G4381A Thermal Separation Probe (TSP), and a 30 m x 0.25 mm DB-5MS capillary column (25 μ m film thickness). Liquid samples (typically 1 μ L) were introduced to the column *via* split mode injection with a 50:1 split ratio. The set temperatures were 220 °C for the GC injection port, 280 °C for the MSD transfer line, 230 °C for the MS source, and 150 °C for the MS quad. The energy of the EI source was set to 69.9 eV. For GC analyses, the oven temperature was set at an initial temperature of 60 °C for 2.25 min, then ramped to 225 °C at 3 °C min⁻¹ and held at this final temperature for 3 min. The system used helium flowing at a rate of 3.0 mL min⁻¹ as the mobile phase. The method used a 3-minute solvent delay. Solid samples were introduced into the instrument using the TSP. After the TSP was pre-heated to the set temperature, the sample carrier was inserted into the probe, which was connected directly to the MSD transfer line by a deactivated quartz capillary. Helium flowing at a rate of 3.0 mL min⁻¹ was used as carrier. Data analysis was performed using Agilent MassHunter Qualitative Analysis Navigator.

Infrared Spectroscopy

Routine small molecule FTIR spectra were collected on an Agilent Cary 630 FTIR instrument equipped with a single-reflection germanium attenuated total reflectance (ATR) module. The instrument was calibrated before sampling against a newly cleaned (acetone) and dried crystal surface. Solid samples were placed directly on the crystal and secured with a needle press. 512 scans from 4000 to 600 cm⁻¹ were recorded. A background was collected for each sample (512 scans).

Melting Points

Melting points were determined with a Mettler Toledo MP50 Melting Point System. The samples were placed in capillary tubes, which were inserted into the heating block. The heating block was then heated at $1\text{ }^{\circ}\text{C min}^{-1}$.

Transmission Electron Microscopy

Analyte dispersions were prepared by sonicating in a Branson CPX5800H ultrasonic bath. Prior to sample preparation, 200-Cu C-B grids or pure carbon film grids were plasma-treated for 30 seconds using an Emitech K100x glow discharger. $5\text{ }\mu\text{L}$ of sample dispersion was added to the grid and allowed to absorb for 5 minutes before the excess solvent was wicked.

The grid was then transferred to a single-tilt sample holder and imaged on an FEI Tecnai 20 TEM operating at 200 kV. Images were recorded on a Tvips F416. Data was collected using SerialEM software. Tilting was performed with the equipped alpha-rotation goniometer. SAED patterns were recorded on an FEI Tecnai 20 TEM using a $40\text{ }\mu\text{m}$ aperture. The obtained patterns were calibrated against the (111) planes of evaporated aluminum (plane spacing $.2338\text{ nm}$) on a 3 mm grid. The calibration sample was purchased from Electron Microscopy Sciences (EMS p/n 80044).

Atomic Force Microscopy

AFM images were obtained on a Veeco Dimension 3100 atomic force microscope in tapping mode using NanoScope Analysis software or a Park Systems NX10 system. Silicon cantilevers were obtained from Bruker (NCHV-A, $k = 40\text{ N/m}$; $f_0 = 320\text{ kHz}$). The samples were prepared by drop casting $\sim 0.01\text{ mg/mL}$ solution in hexanes onto a mica disc, then wicking away the excess. The mica disks were then allowed to dry at room temperature for 24 hours. Gwyddion 2.60 was used for data analysis and visualization of AFM images.

X-ray Photoelectron Spectroscopy

Samples were spread onto double-sided copper tape for XPS analysis. Surveys and high-resolution spectra were acquired on a PHI VersaProbe II Scanning XPS Microprobe using a monochromatic Al X-ray at pressures of 10^{-10} to 10^{-7} Torr. The data was smoothed by using the Savitzky-Golay method, with a smoothing width of five, and analyzed using CasaXPS.^{1, 2}

For the analysis of high resolution data, a Tougaard background³ was applied to each peak before deconvolution. All peak fits used generalized Voigt-like peak shapes, as this function is most appropriate for fitting asymmetric XPS signals.⁴ CasaXPS provides a generalized Voigt function described as Lorentzian Finite: $\text{LF}(\alpha, \beta, w, n, m)$, where the first three parameters (α, β, w) affect the Lorentzian line shape and its asymmetry and the final two (n, m) change the width of the Gaussian function and the number of times convolution with the Lorentzian component occurs.⁵ Symmetrical peak parameters for the LF line shape were used: $\text{LF}(1, 1, 255, 360, 6)$, values derived from default symmetric peak shape settings for CasaXPS. All sub-peak widths were constrained to full width at half maximum (FWHM) of 1.6 eV or less. The residual Br 3d peaks were deconvolved to two distinctive species: Br covalently bonded to sp^2 carbon (71.4, 70.5 eV),⁶⁻⁸ corresponding to partially unreacted sites, and weakly coordinated/anionic Br (67.5-69.5 eV)⁸⁻¹² trapped within the carbon matrix or on the edges or surfaces of γ -graphyne sheets. All peaks were allowed a $\pm 0.2\text{ eV}$ padding to the peak position.

Thermogravimetric Analysis

TGA was carried out on a TA Instruments Q500. 5-10 mg of the sample was loaded in a platinum pan and was heated from 30 to 300 $^{\circ}\text{C}$ at a ramp of 10°C/min using nitrogen as the purge gas (flow rate 40 mL min^{-1}).

Differential Scanning Calorimetry

DSC was performed using a TA Instruments DSC model Q100 and Q250. Heating rate was $5^{\circ}\text{C min}^{-1}$ and nitrogen flow rate was set to 60 mL min^{-1} . 5-10 mg of the sample was placed in a sealed aluminum pan and heated from 40°C to the temperature at which 5% mass is lost based on the prior TGA measurement ($T_{5\%}$), 350°C for edge-modified graphynes.

UV-Vis Spectroscopy

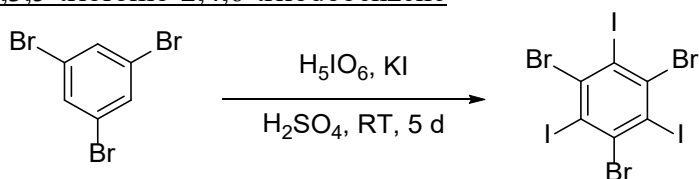
The UV-Vis spectra were recorded by a Lambda XLS+ spectrometer (PerkinElmer, Waltham, MA) with a scanning range from 200 to 950 nm using a glass cuvette (Hellma, Germany). The optical path length was 10 mm.

SAED Simulation

The lattice parameters and bond lengths of γ -graphyne were obtained from previously published studies.^{13, 14} SAED simulations were performed using the CrystalMaker software suite.¹⁵ A model of a single γ -graphyne sheet was built in CrystalMaker using a hexagonal P6 lattice with parameters a and c set to 6.86 \AA and 3.4 \AA , respectively. The asymmetric unit comprised four atoms placed at 0.208, 0.412, 0.589, 0.795 along the hexagonal P6 x axis. The basic models corresponding to various sheet stacking modes were constructed and visualized using Vesta.¹⁶

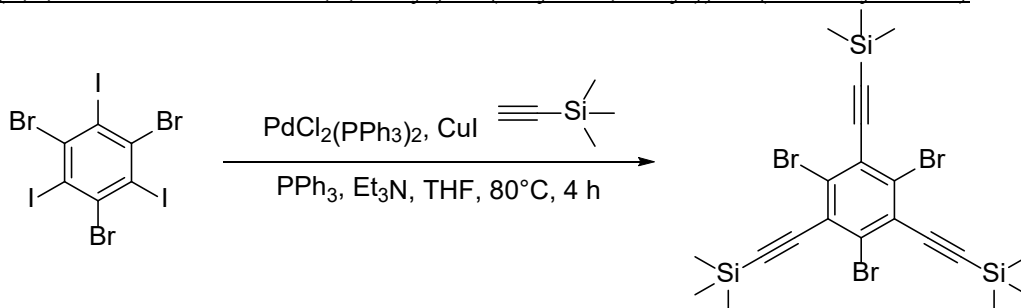
3. Synthesis of small molecules

1,3,5-tribromo-2,4,6-triiodobenzene



To concentrated H_2SO_4 (500 mL) at room temperature was added periodic acid (41.03 g, 180 mmol) in small portions over 15 min. After dissolution of the periodic acid, crushed KI (89.64 g, 540 mmol) was added in small portions at $0\text{ }^\circ\text{C}$ over 1 h. To the resulting deep purple solution at $0\text{ }^\circ\text{C}$ was added 1,3,5-tribromobenzene (18.89 g, 60.0 mmol) in small portions over 25 min. After the solution was stirred at room temperature for 5 days, the resulting thick mixture was poured onto ice. The resulting precipitate was filtered and washed with H_2O ($5 \times 400\text{ mL}$) and then MeOH ($5 \times 400\text{ mL}$) to give 1,3,5-tribromo-2,4,6-triiodobenzene (42 g) as a light cream solid. The substance was dissolved in *N*-methyl-2-pyrrolidone (250 mL) under heating to $50\text{ }^\circ\text{C}$, after which ethanol was added slowly until solids began to precipitate. The mixture was left at room temperature overnight, then the solids were filtered and washed with ethanol ($3 \times 100\text{ mL}$). The solid was dried under high vacuum for 3 days to give 1,3,5-tribromo-2,4,6-triiodobenzene (30 g, 72%) as a pale-yellow solid. FTIR (neat) $\nu_{\text{max}} = 1488, 1354, 1262, 1227, 1147, 1002, 858, 771, 739, 554, 508\text{ cm}^{-1}$. ^1H NMR (500 MHz, DMSO- d_6) no signal. ^{13}C NMR (126 MHz, DMSO- d_6) δ 138.61 (CBr), 108.23 (CI). EI-MS fragmentation: m/z 695.5, 693.5, 691.5, 689.5, 567.6, 566.6, 565.6, 564.6, 439.7, 437.6.

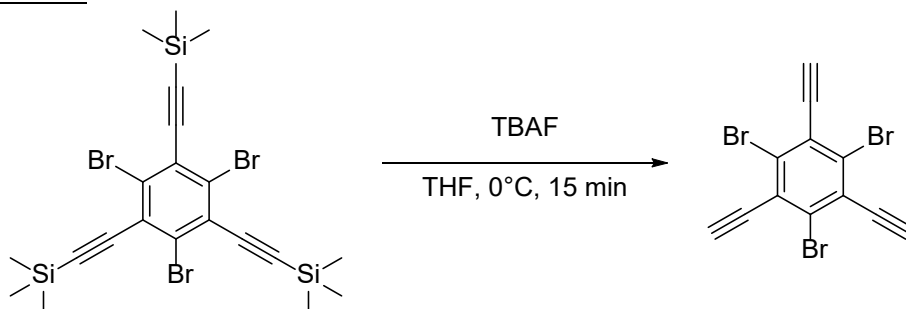
((2,4,6-tribromobenzene-1,3,5-triyl)tris(ethyne-2,1-diyl))tris(trimethylsilane)



1,3,5-tribromo-2,4,6-triiodobenzene (6.92 g, 10 mmol), $[\text{PdCl}_2(\text{PPh}_3)_2]$ (2.81 g, 4 mmol, 40 mol%), CuI (381 mg, 2 mmol, 20 mol%), TEA (500 mL) and THF (400 mL) were added to a dry three-necked flask. Ethynyltrimethylsilane (14.73 g, 21.4 mL, 150 mmol) and Ph_3P (1.31 g, 5 mmol, 50 mol%) were added to the mixture. The mixture was stirred at $80\text{ }^\circ\text{C}$ for 4 h under argon. After the removal of solvent on a rotary evaporator, DCM (300 mL) was added to the residue and filtered through Celite. The mixture was washed with water ($2 \times 100\text{ mL}$) dried over anhydrous Na_2SO_4 , filtered through pad of silica gel and the solvent was removed under reduced pressure. The residue was further purified by flash chromatography using *n*-hexane as the eluent to yield the product as a yellow solid (2.64 g, 4.38 mmol, yield: 44%). The product was then recrystallized from acetonitrile to yield ((2,4,6-tribromobenzene-1,3,5-triyl)tris(ethyne-2,1-diyl))tris(trimethylsilane) as a white solid (1.9 g, 3.15 mmol, yield: 32%). R_f (hexanes) = 0.16. Mp = $141.9\text{ }^\circ\text{C}$ (after recrystallization from acetonitrile). FTIR (neat) $\nu_{\text{max}} = 2958, 2160, 1376, 1340, 1245, 1019, 834, 758, 708, 658, 633, 539\text{ cm}^{-1}$. ^1H NMR (500 MHz, CDCl_3): $\delta = 0.29$ [s, 27H

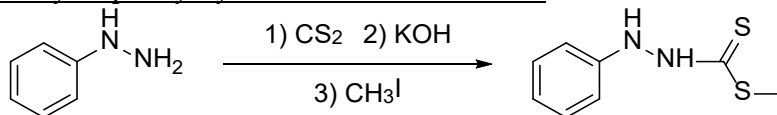
Si(CH₃)₃] ppm. ¹³C NMR (126 MHz, CDCl₃): δ 129.09 (CBr), 127.49 (C₆C≡C), 106.79 (C≡CSi), 101.83 (C₆C≡C), -0.23 [Si(CH₃)₃] ppm. ²⁹Si NMR (99 MHz, CDCl₃) δ -15.87 ppm. EI-MS fragmentation: m/z 603.9, 602, 601.9, 590.9, 589.9, 588.9, 587.9, 586.9, 584.9.

TBTEB



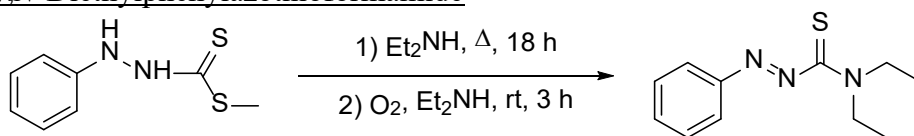
To a solution of ((2,4,6-tribromobenzene-1,3,5-triyl)tris(ethyne-2,1-diyl))tris(trimethylsilane) (1.81 g, 3 mmol) in THF (40 mL) was added 6.58 mL TBAF (75% solution in water, 18 mmol) and stirred at 0 °C for 15 min. The solution was then diluted with ethyl acetate and washed with distilled water and dried with anhydrous Na₂SO₄. The solvent was removed on a rotary evaporator. The residue was further purified by flash chromatography using n-hexane as the eluent to give TBTEB as a white solid (950 mg, 2.46 mmol, yield: 82%). R_f (hexanes) = 0.17. Mp = decomposition after 150 °C. FTIR (neat) ν_{max} = 3275, 2922, 2112, 1519, 1368, 1336, 965, 736, 681, 634 cm⁻¹. ¹H NMR (500 MHz, CDCl₃): δ = 5.16 (s, 3H, (C≡CH) ppm. ¹³C NMR (126 MHz, CDCl₃): δ 129.89 (CBr), 126.33 (C₆C≡CH), 91.85 (C≡CH), 80.96 (C₆C≡CH) ppm. EI-MS fragmentation: m/z 390.8, 389.9, 388.8, 387.8, 386.8, 385.8, 384.8, 383.8.

Methyl 2-phenylhydrazine-1-carbodithioate



The synthetic procedure of methyl 2-phenylhydrazine-1-carbodithioate was adapted from literature¹⁷. Ethanol (750 mL) was placed in a 2-liter three-necked round-bottom flask. Phenylhydrazine (43.3 g, 39.4 mL, 400 mmol) was added, and the solution was stirred under argon. Carbon disulfide (34.1 g, 27.6 mL, 450 mmol) was added dropwise over 15 minutes. A thick, colorless precipitate formed. After the mixture had been stirred for an additional 30 minutes, potassium hydroxide (30.4 g, 460 mmol) in ethanol (200 mL) was added. The precipitate dissolved, and the color changed to orange. The solution was stirred for an additional 30 minutes. Methyl iodide (65.3 g, 28.6 mL, 460 mmol) was added, and a nearly white solid (KI) was formed. The solution was stirred for an additional 30 minutes. The solvent was removed by evaporation. The resulting substance was dissolved in dichloromethane (DCM, 400 mL) and washed with water (3 × 100 mL), then dried with Na₂SO₄ and evaporated. A red oil was obtained. The product was dissolved in DCM (100 mL), and hexanes (1 L) were added to the solution. The resulting white solid was filtered and dried under vacuum for 1 day to yield methyl 2-phenylhydrazine-1-carbodithioate (42.3 g, 213 mmol, 53% yield). ¹H NMR (500 MHz, CDCl₃) δ 8.88 (s, 1H, NH-C(S)), 7.31 (t, *J* = 7.8 Hz, 2H CH_{aryl}), 7.01 (t, *J* = 7.4 Hz, 1H, CH_{aryl}), 6.85 (d, *J* = 8.0 Hz, 2H, CH_{aryl}), 6.07 (s, 1H, PhNH), 2.59 (s, 3H, SCH₃). ¹³C NMR (126 MHz, CDCl₃) δ 208.39 (C(S)S), 145.31 (C_{q, aryl}), 129.65 (CH_{aryl}), 122.35 (CH_{aryl}), 113.36 (CH_{aryl}), 17.60 (CH₃).

N,N-Diethylphenylazothioformamide



The synthetic procedure of *N,N*-Diethylphenylazothioformamide was adapted from literature¹⁷ and the substance was purified using the literature method¹⁸. Methyl 2-phenylhydrazine-1-carbodithioate (41.6 g, 210 mmol) was placed in a 1-liter three-necked round-bottom flask. To this flask, diethylamine (200 mL) was added. The resulting solution was refluxed for 18 hours under an argon atmosphere. After 18 hours, the reaction was terminated as confirmed by ¹H NMR analysis, which indicated complete conversion to 4,4-diethyl-1-phenylthiosemicarbazide. ¹H NMR (500 MHz, CDCl₃) δ 7.28 (dd, *J* = 8.6, 7.4 Hz, 1H, CH_{aryl}), 6.98 – 6.90 (m, 3H, CH_{aryl}), 3.70 (q, *J* = 7.2 Hz, 4H, CH₂), 1.28 (t, *J* = 7.1 Hz, 6H, CH₃).

After the completion of the reflux step, the solution was exposed to oxygen in the form of air at room temperature for 3 hours. The progress of the reaction was monitored using NMR analysis. Subsequently, the solution was concentrated to obtain a dense red oil (yield 100%). To purify the oil, recrystallization was performed using 20:1 heptane: ethyl acetate (2 L). The recrystallization process was carried out in a dry ice acetone bath. As a result, red crystals (38.9 g, yield 84%) were obtained. The second crystallization process produced orange crystals of *N,N*-diethylphenylazothioformamide (30.6 g, yield 66%). Mp = 56.4 °C. FTIR (neat) ν_{max} = 2978, 2950, 1554, 1498, 1470, 1392, 1169, 812 cm⁻¹. ¹H NMR (500 MHz, CDCl₃) δ 7.90 (dd, *J* = 8.0, 1.8 Hz, 1H, CH_{aryl}), 7.57 – 7.50 (m, 3H, CH_{aryl}), 4.03 (q, *J* = 7.1 Hz, 2H, CH₂), 3.52 (q, *J* = 7.2 Hz, 2H, CH₂), 1.41 (t, *J* = 7.2 Hz, 3H, CH₃), 1.19 (t, *J* = 6.4 Hz, 3H, CH₃). ¹³C NMR (126 MHz, CDCl₃) δ 194.17 (C(S)), 151.84 (C_{q, aryl}), 132.77 (CH_{aryl}), 129.36 (2C, CH_{aryl}), 123.66 (2C, CH_{aryl}), 47.87 (CH₂), 45.20 (CH₂), 13.81 (CH₃), 11.52 (CH₃).

4. Synthesis of Carbon Materials

General Synthetic Procedure for γ -Graphyne (GY-Br)

1,3,5-Tribromo-2,4,6-triethynylbenzene (96.7 mg, 0.25 mmol), Pd(PPh₃)₄ (289 mg, 0.25 mmol) and CuI (3.8 mg, 0.02 mmol) were placed in a Schlenk flask under argon atmosphere and pyridine (50 mL) was added. The tube was sealed, and the contents degassed by three freeze-pump thaw cycles. The reaction mixture was stirred under argon atmosphere at 110 °C for 72 h. The reaction mixture was concentrated by a rotary evaporator. Solution of *N,N*-diethyl-2-phenyldiazene-1-carbothioamide in toluene (50 mL, 0.3% mass, 150 mg of *N,N*-diethyl-2-phenyldiazene-1-carbothioamide) was added to the mixture and then was stirring for 3 hours. Then the solid was filtrated. The solid product was washed with toluene, ethyl acetate, water, isopropanol, ethanol, methanol and acetone (each 200 ml). Then the residue was dried under high vacuum for 1 day to give the black solid.

It must be emphasized that the quality of tetrakis(triphenylphospine)palladium(0) catalyst has a significant impact on the success of the polymerization of TBTEB. The catalyst must be golden-yellow in coloration. Dark orange, brown, or greenish batches of the catalyst result in incomplete polymerization, which can be diagnosed through observing an intense IR peak for the unreacted terminal alkynes at $\sim 2100\text{ cm}^{-1}$.

Edge Functionalization of GY-Br in One Pot by Sonogashira Coupling

1,3,5-Tribromo-2,4,6-triethynylbenzene (58 mg, 0.15 mmol), Pd(PPh₃)₄ (173 mg, 0.15 mmol) and CuI (2.3 mg, 0.012 mmol) were placed in a Schlenk flask under argon atmosphere and pyridine (30 mL) was added. The tube was sealed, and the contents degassed by three freeze-pump thaw cycles. The reaction mixture was stirred under argon atmosphere at 80 °C for 24 h. After 24 hours phenylacetylene (92 mg, 0.1 mL, 0.9 mmol) was added to the reaction mixture. The reaction mixture was stirred under argon atmosphere at 80 °C for 24 h. The solid product was washed with toluene, ethyl acetate, water, isopropanol, ethanol, methanol and acetone (each 100 ml). Then the residue was dried under high vacuum for 1 day to give the black solid. In some cases, the mixture was further washed to remove palladium: *N,N*-diethyl-2-phenyldiazene-1-carbothioamide (100 mg, 0.45 mmol, 3 equivalents) was added to the mixture and stirred for 3 hours. Then the reaction mixture was evaporated and the solid was filtered. The solid was then washed with acetone, methanol, and toluene 6 times.

Edge Functionalization of GY-Br by CuAAC Click Chemistry

Br-edge γ -graphyne (50 mg), CuI (30 mg), and 1-octadecyl azide (50 mg) were added to a 2-neck flask under argon. Dry THF (40 mL) and DIPEA (5 mL) was added to the flask under argon flow. The reaction mixture was stirred for 48 hours at room temperature. The product was then filtered and washed by water (3 \times 40 mL) and acetone (3 \times 40 mL) and dried under high vacuum for 24 hours to give the black material (41 mg).

5. Characterization

^1H NMR

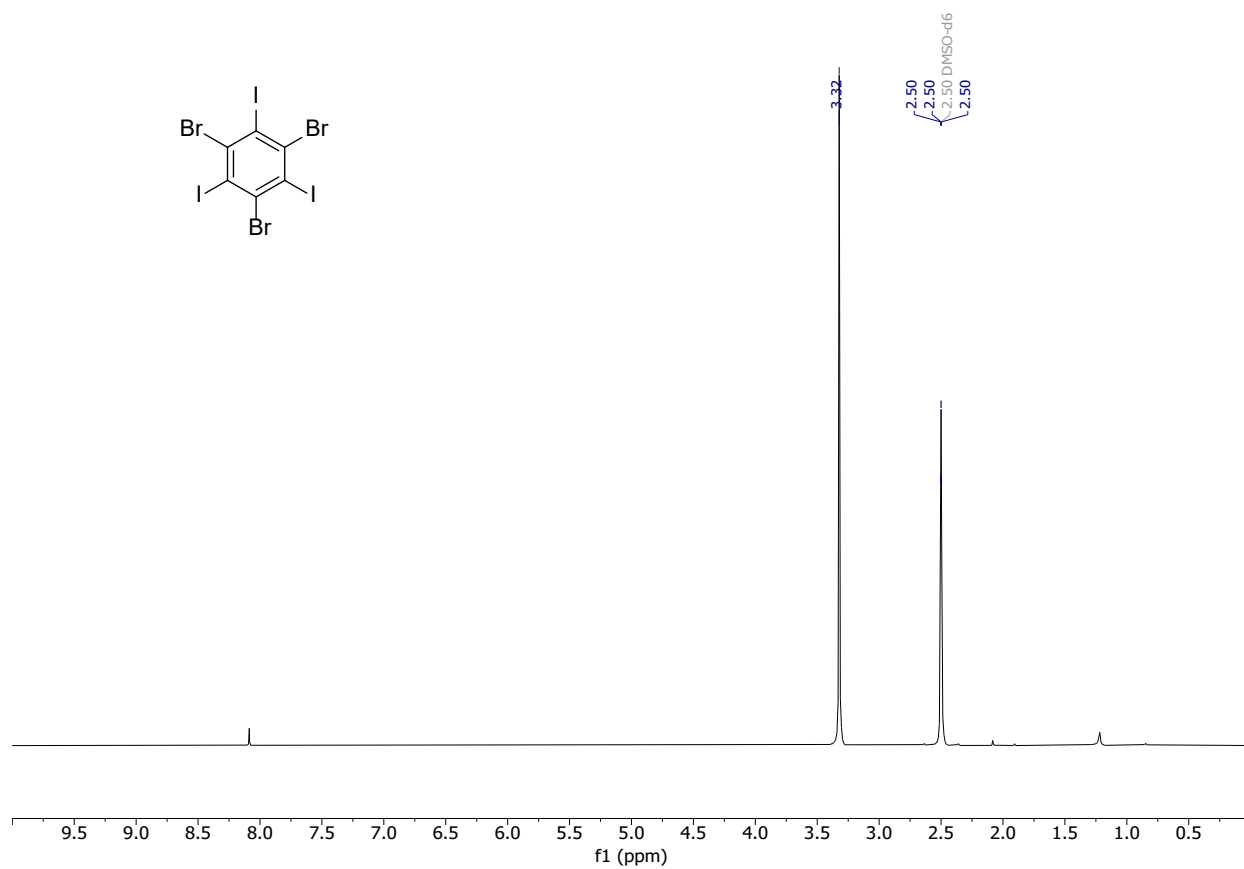


Figure S1. ^1H NMR spectrum of 1,3,5-tribromo-2,4,6-triodobenzene in DMSO- d_6 .

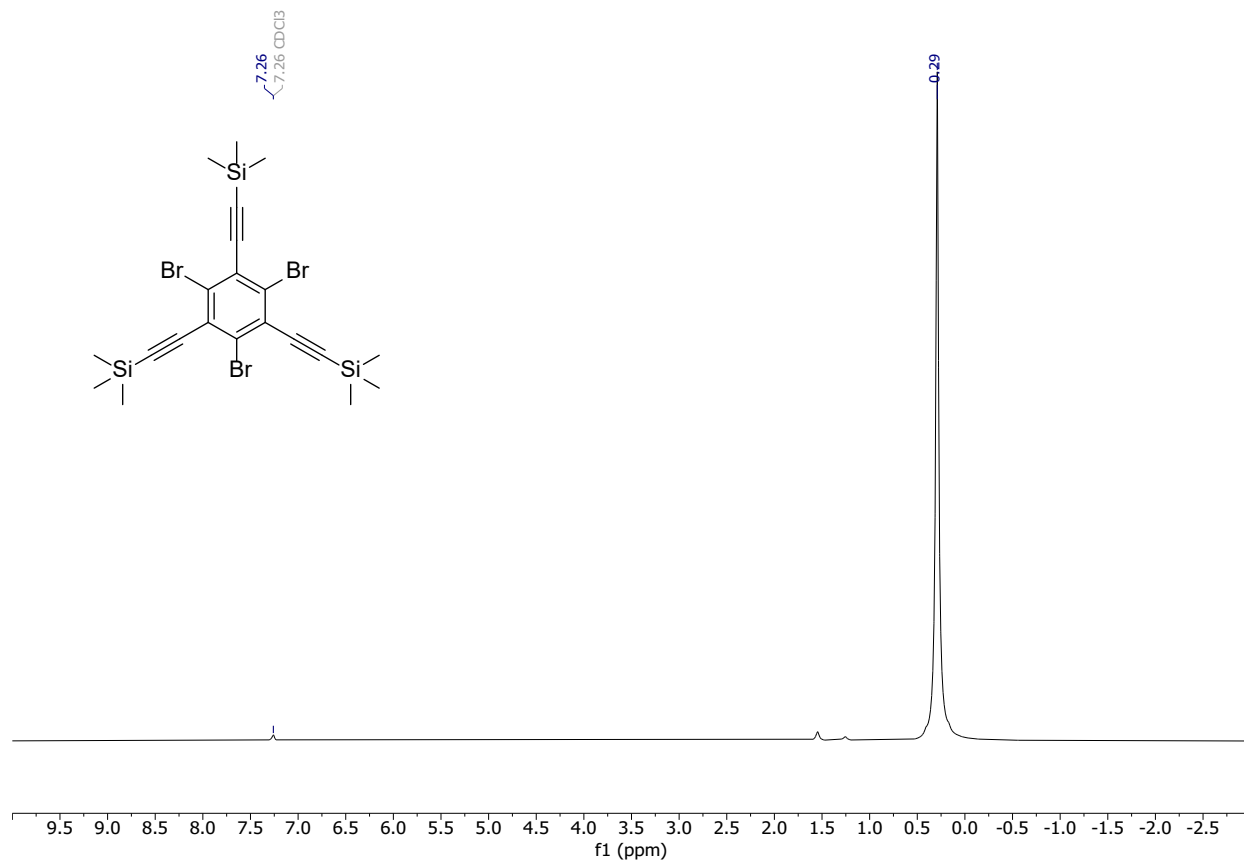


Figure S2. ¹H NMR spectrum of ((2,4,6-tribromobenzene-1,3,5-triyl)tris(ethyne-2,1-diyl))tris(trimethylsilane) in CDCl₃.

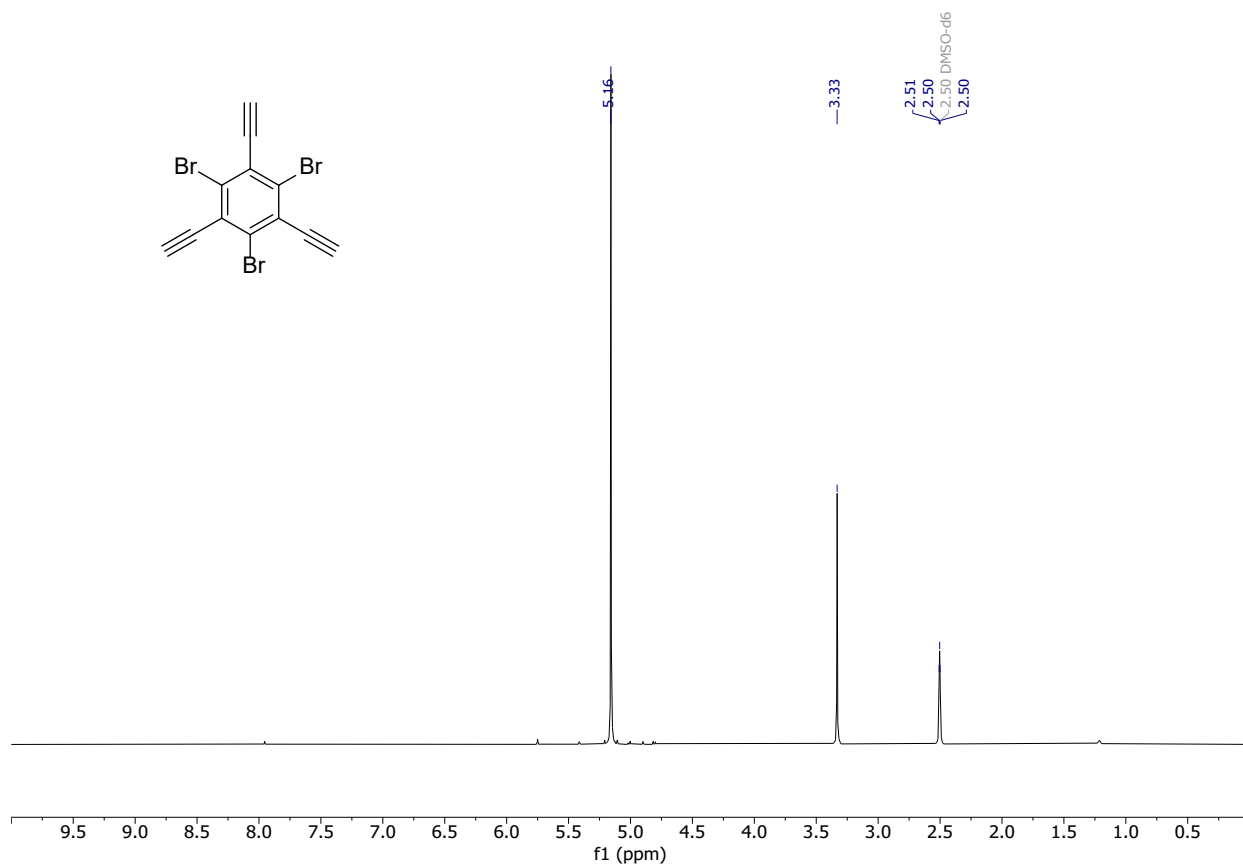


Figure S3. ¹H NMR spectrum of TBTEB in DMSO-d₆.

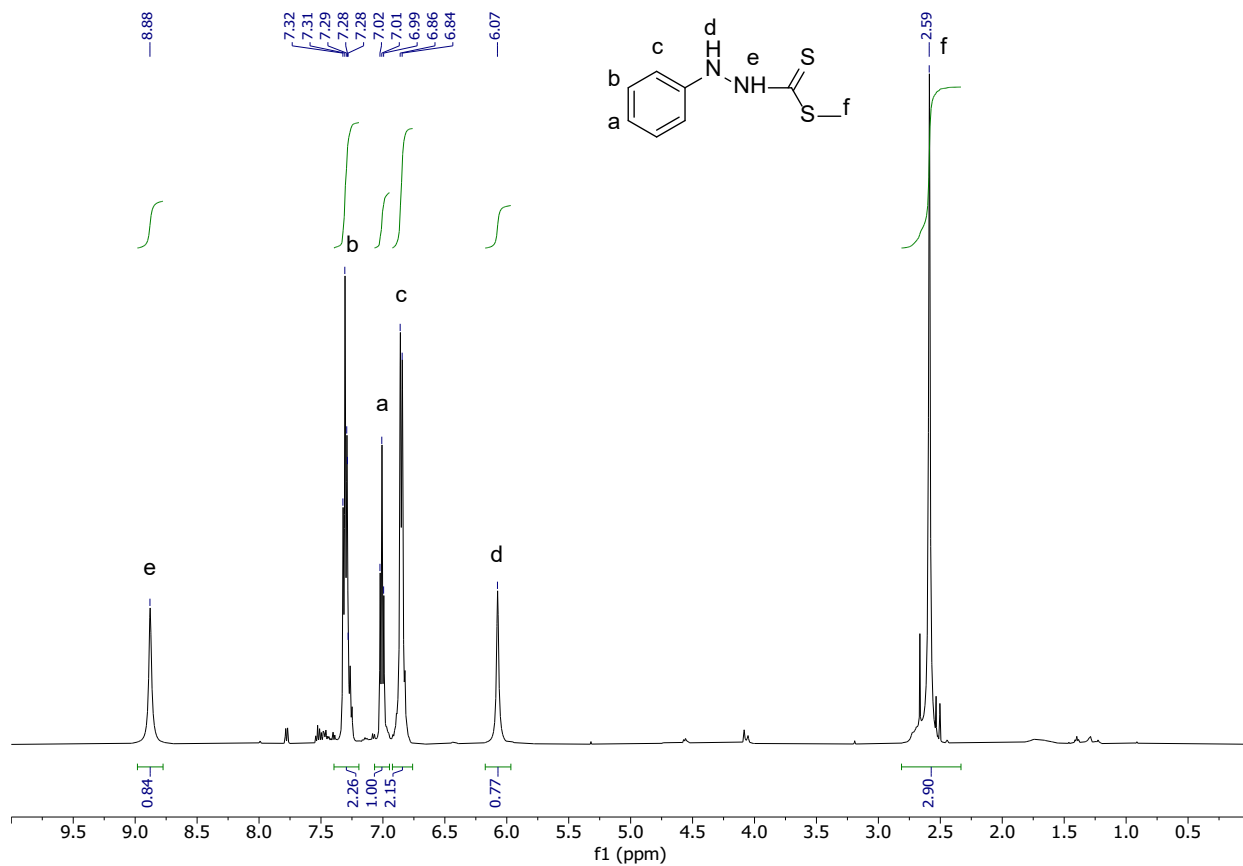


Figure S4. ¹H NMR spectrum of methyl 2-phenylhydrazine-1-carbodithioate in CDCl₃.

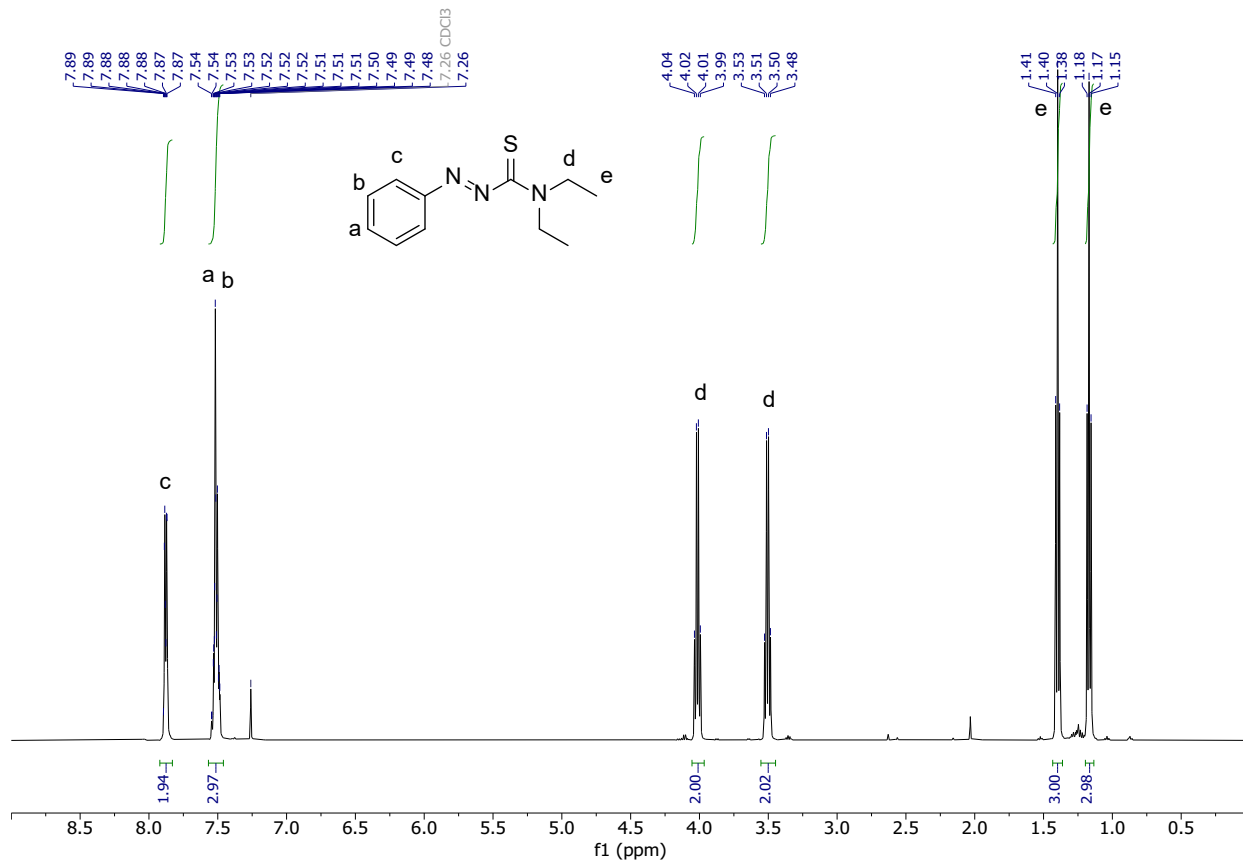


Figure S5. ¹H NMR spectrum of *N,N*-diethylphenylazothioformamide in CDCl₃.

^{13}C NMR

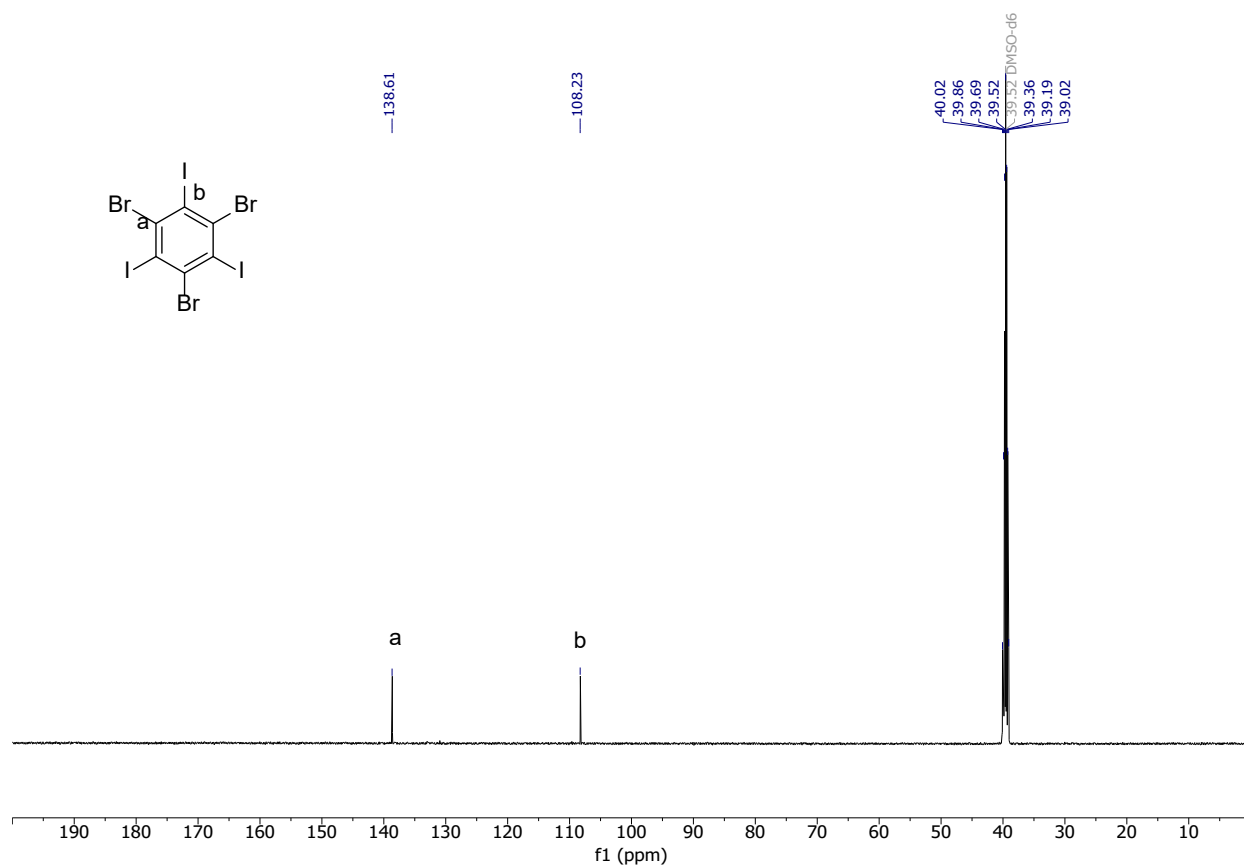


Figure S6. ^{13}C NMR spectrum of 1,3,5-tribromo-2,4,6-triodobenzene in DMSO- d_6 .

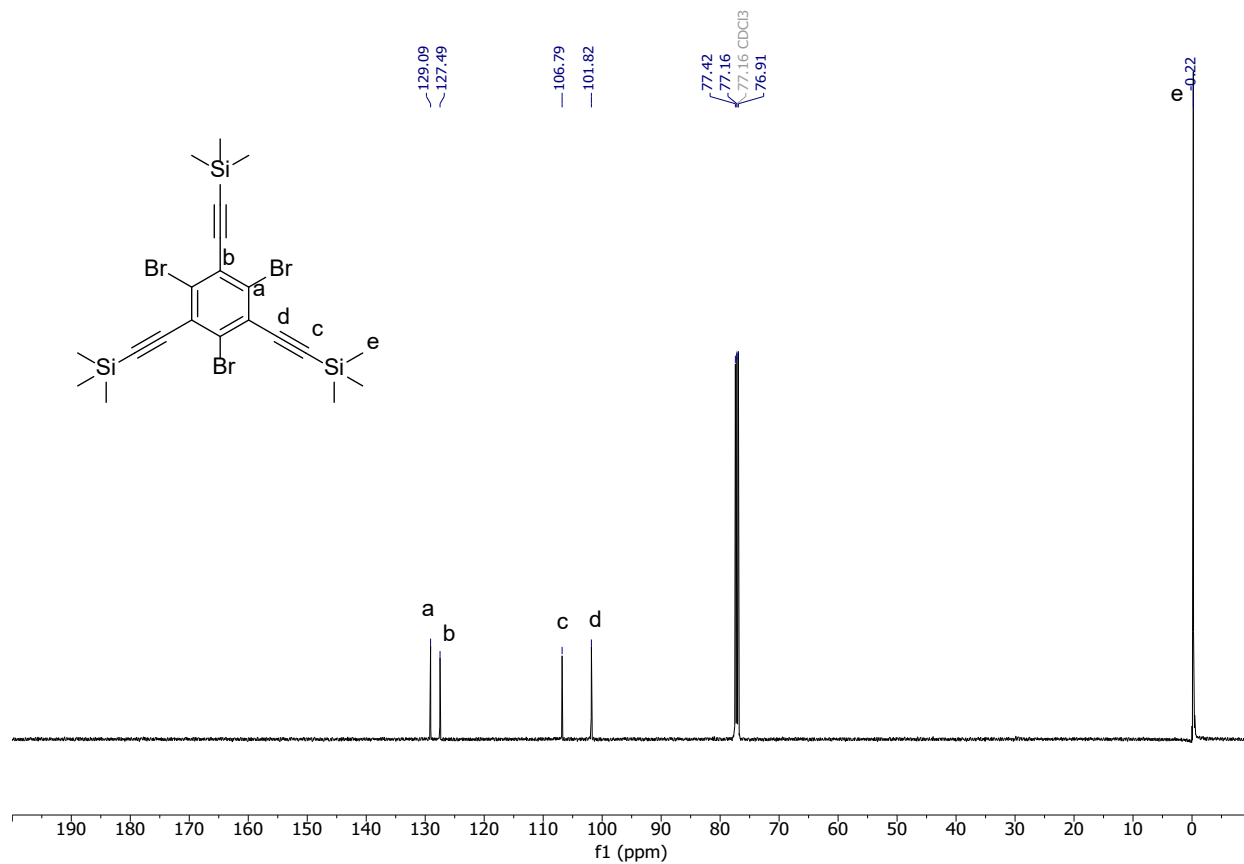


Figure S7. ^{13}C NMR spectrum of ((2,4,6-tribromobenzene-1,3,5-triyl)tris(ethyne-2,1-diyl))tris(trimethylsilane) in CDCl_3 .

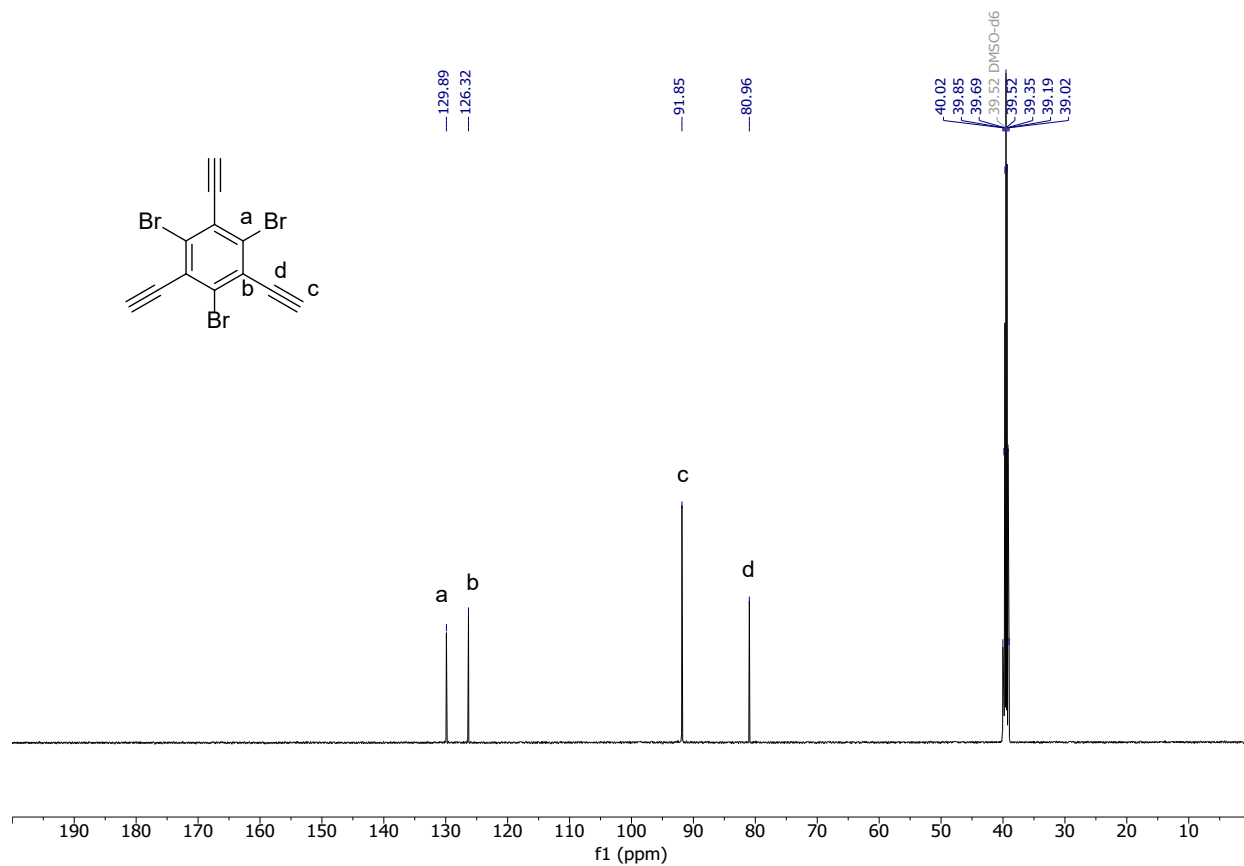


Figure S8. ^{13}C NMR spectrum of TBTEB in DMSO-d_6 .

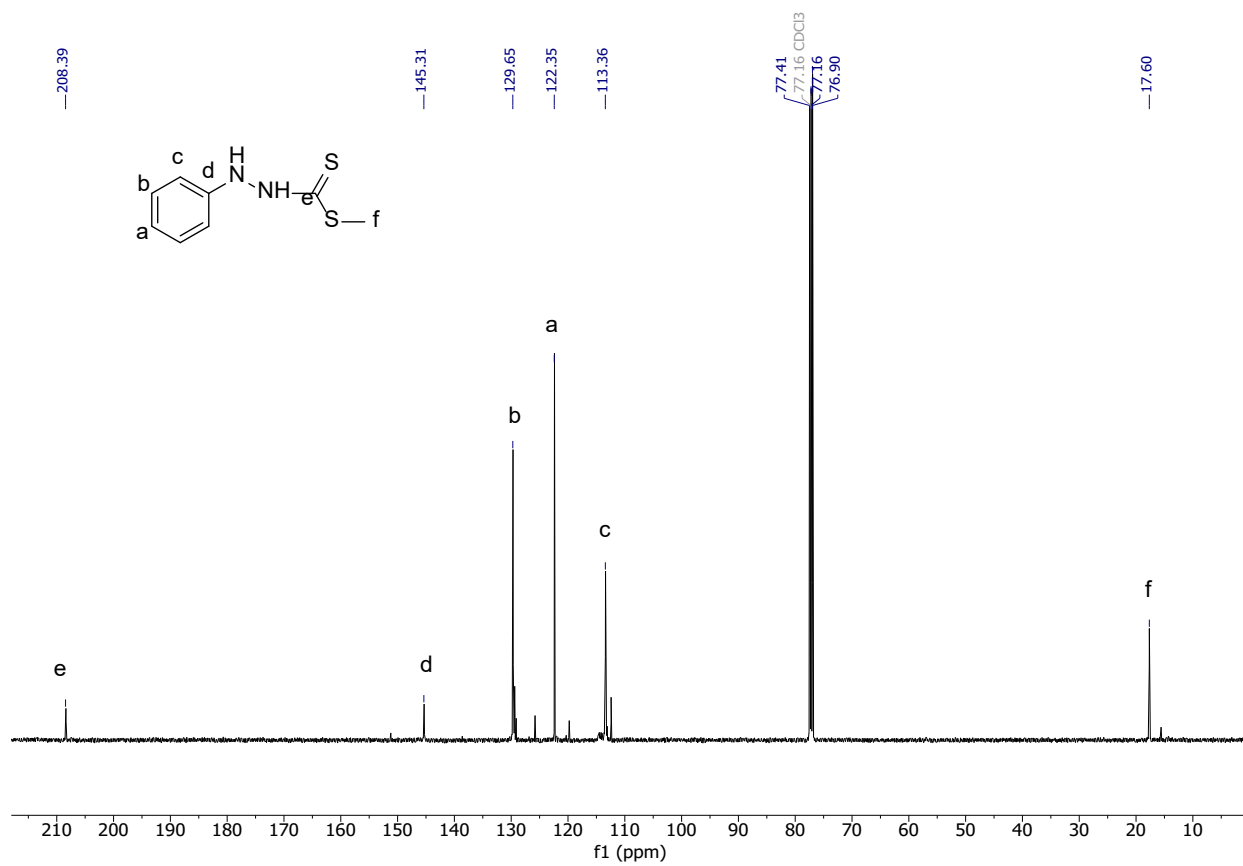


Figure S9. ¹³C NMR spectrum of methyl 2-phenylhydrazine-1-carbodithioate in CDCl₃.

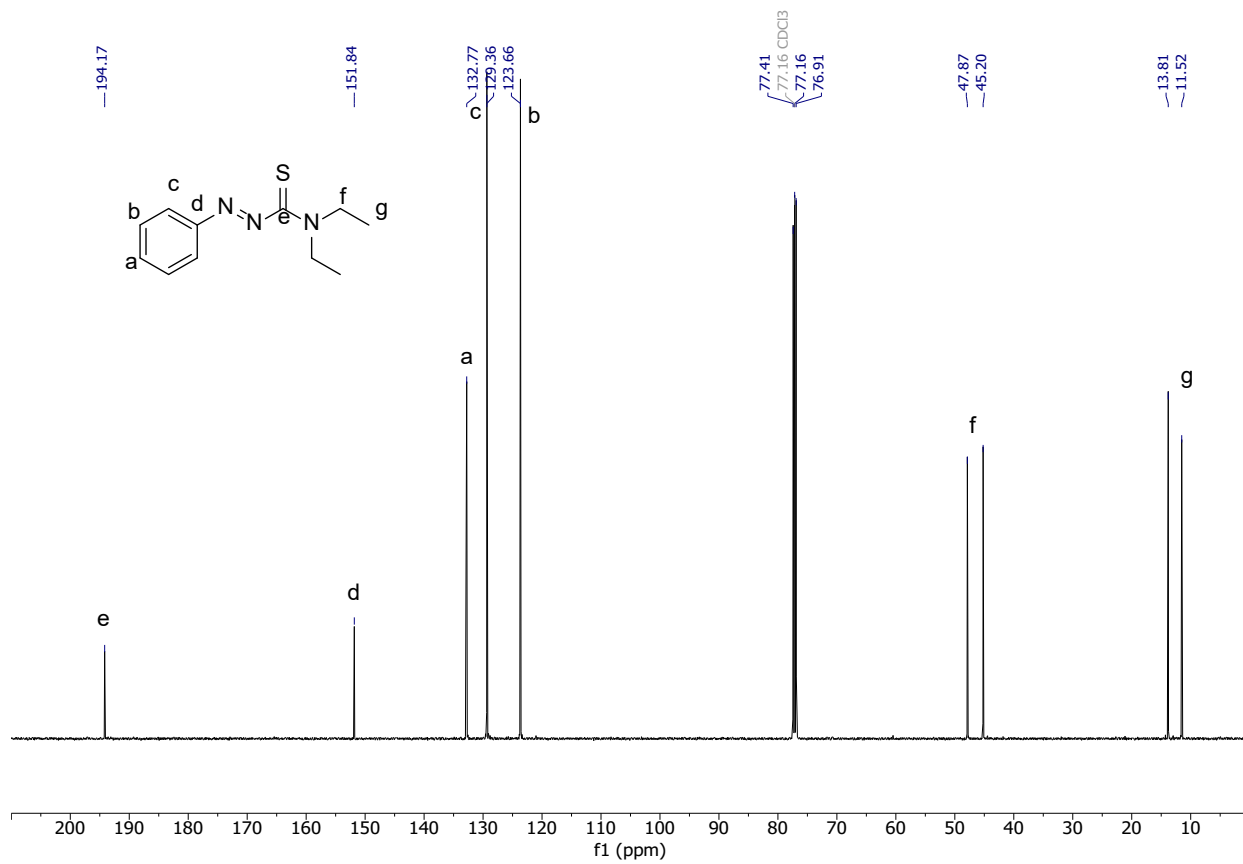


Figure S10. ^{13}C NMR spectrum of *N,N*-Diethylphenylazothioformamide in CDCl_3 .

Mass Spectrometry

The analyses were performed using 2 mg of each functionalized graphyne sample, and 0.1 mg of naphthalene internal reference. The intensity of the naphthalene peak at 128 m/z is normalized to 100 AU in Figures S11-S15.

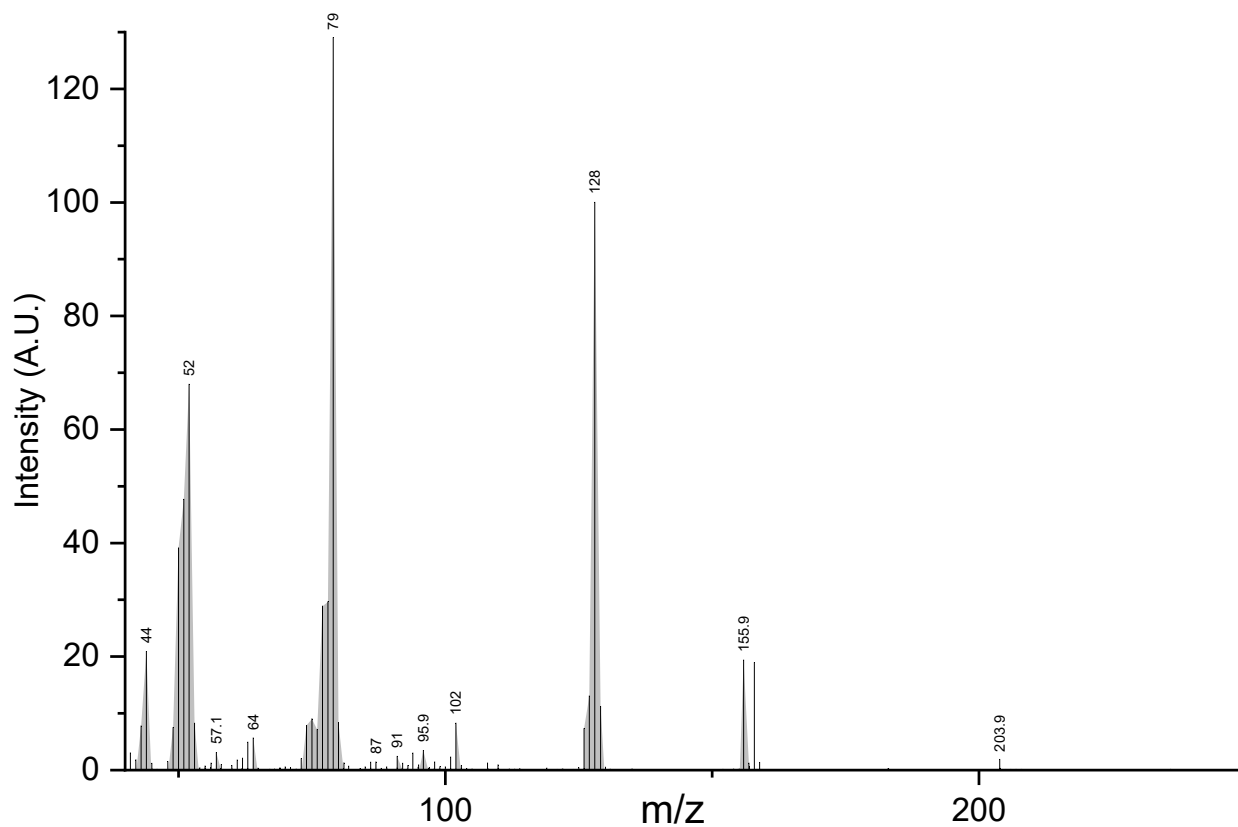


Figure S11. Electron ionization mass spectrum of **GY-Br** volatiles at 290 °C.

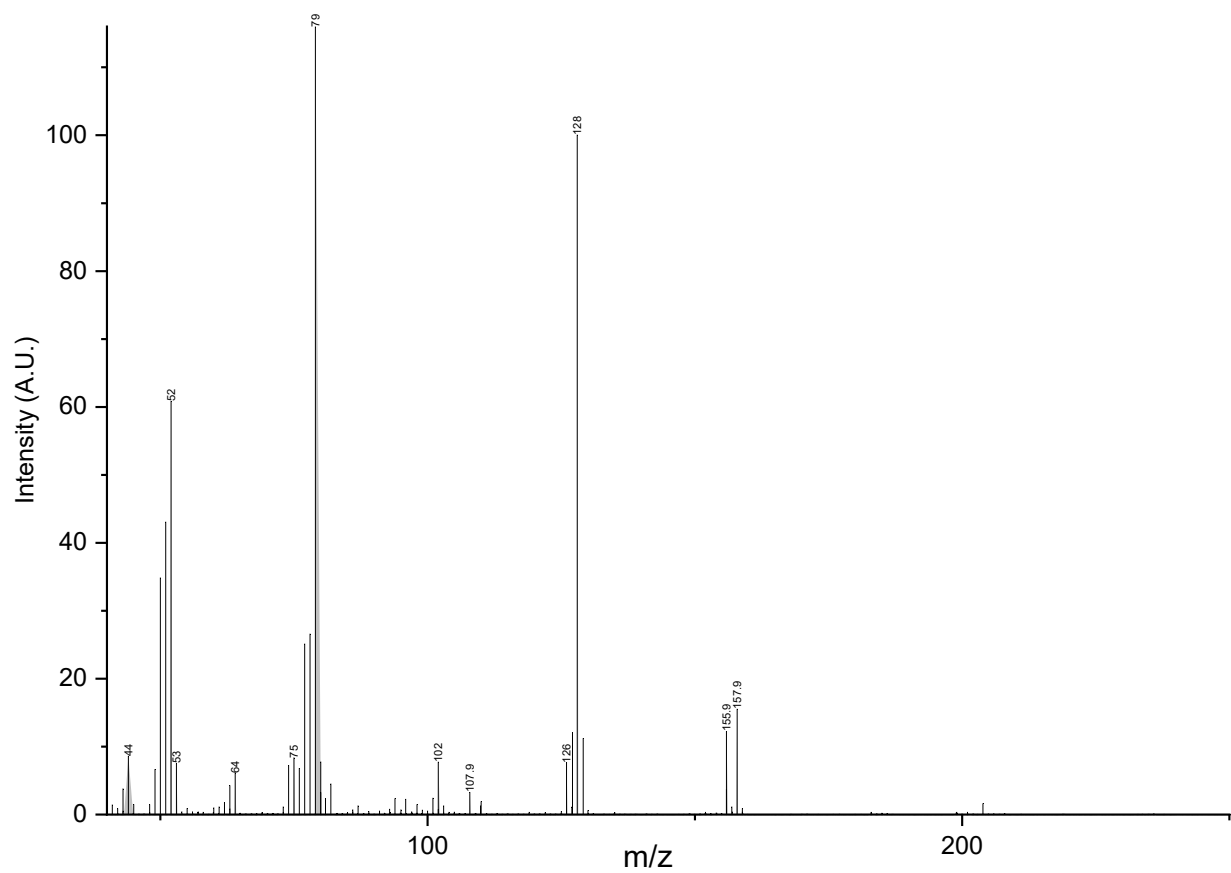


Figure S12. Electron ionization mass spectrum of **GY-Ph** volatiles at 290 °C.

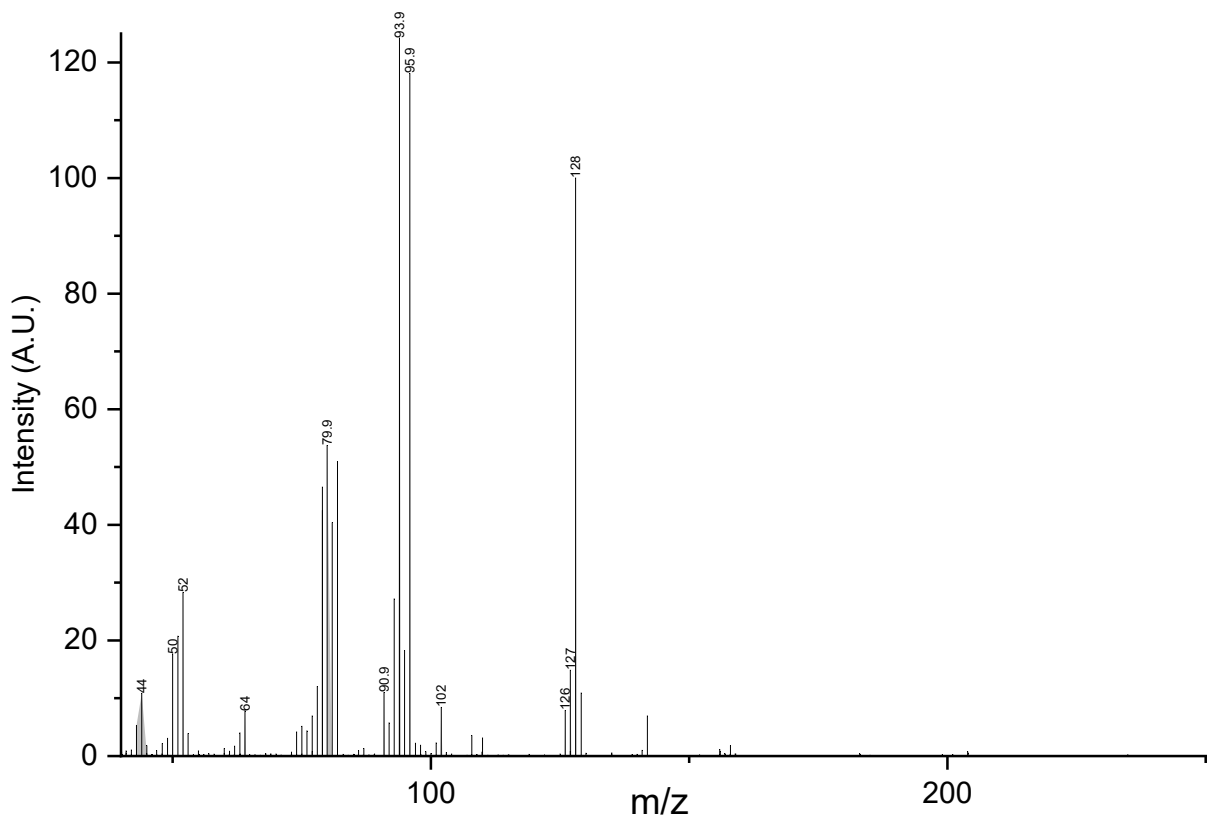


Figure S13. Electron ionization mass spectrum of **GY-MeONaph** volatiles at 290 °C.

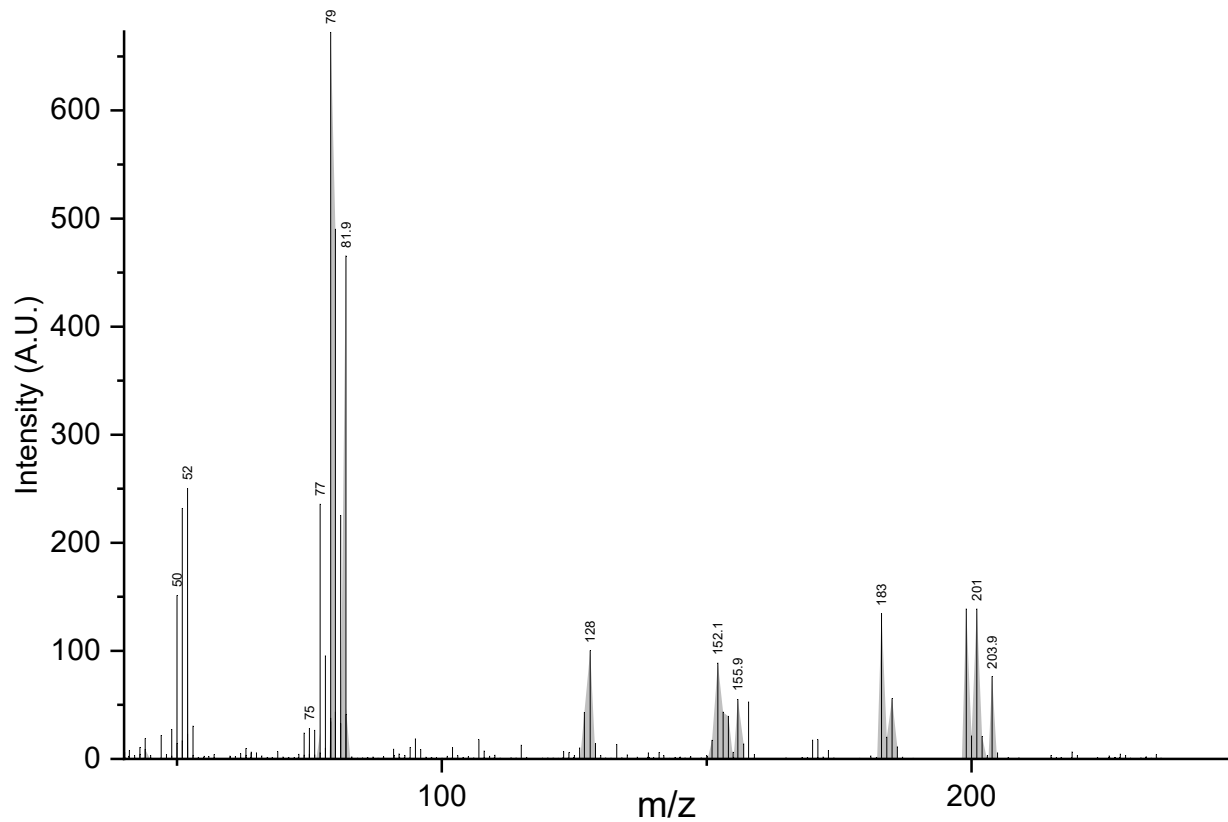


Figure S14. Electron ionization mass spectrum of **GY-C₁₈N₃** volatiles at 290 °C.

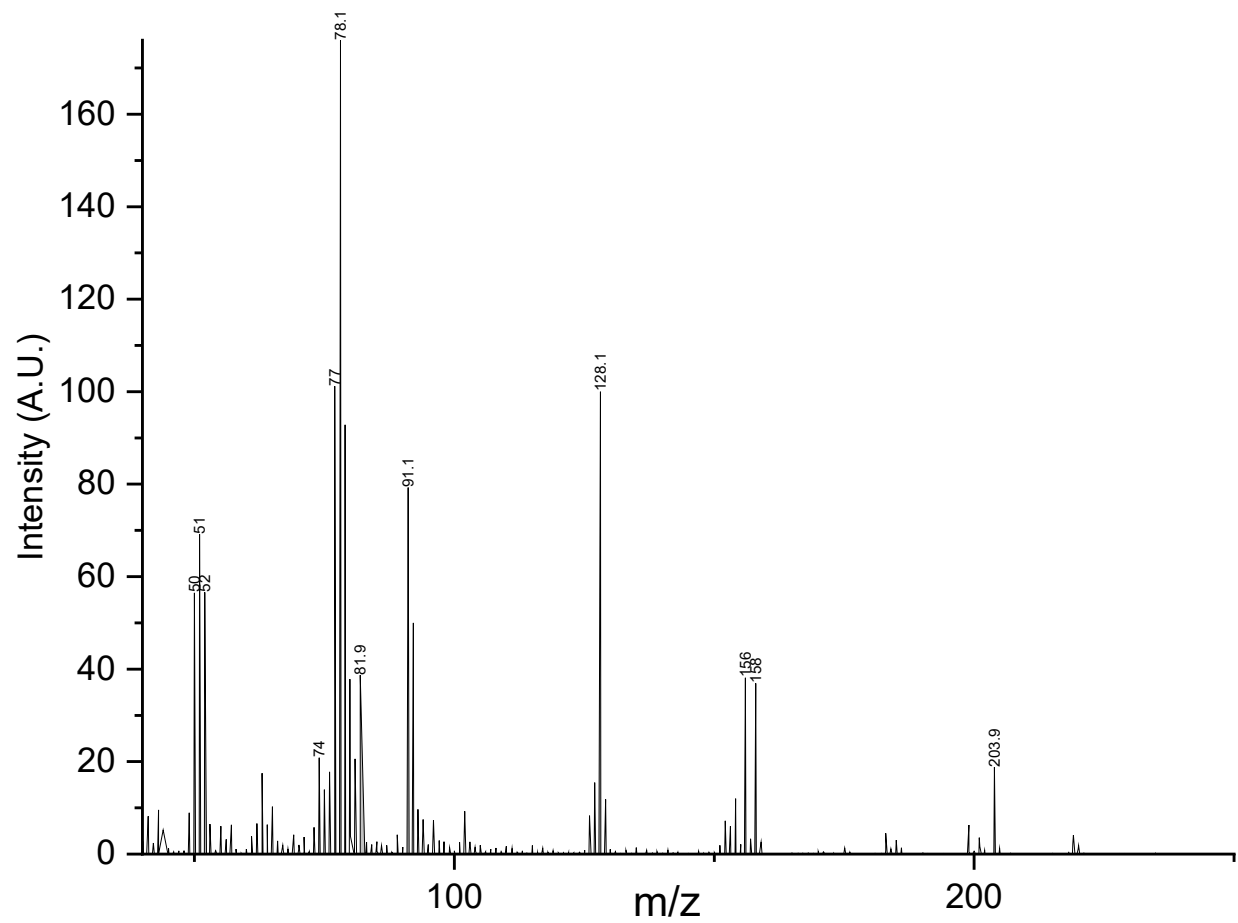


Figure S15. Electron ionization mass spectrum of **GY-C₁₈** volatiles at 290 °C.

XPS

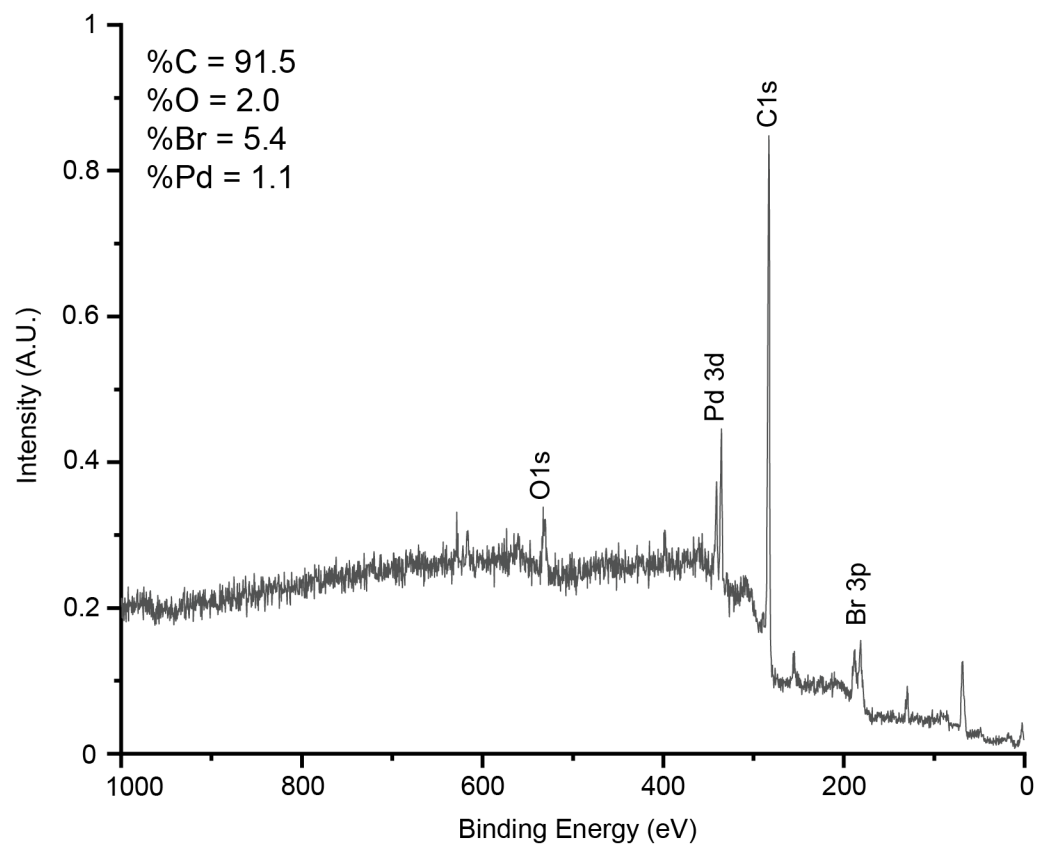


Figure S16. Survey XPS of **GY-Br**

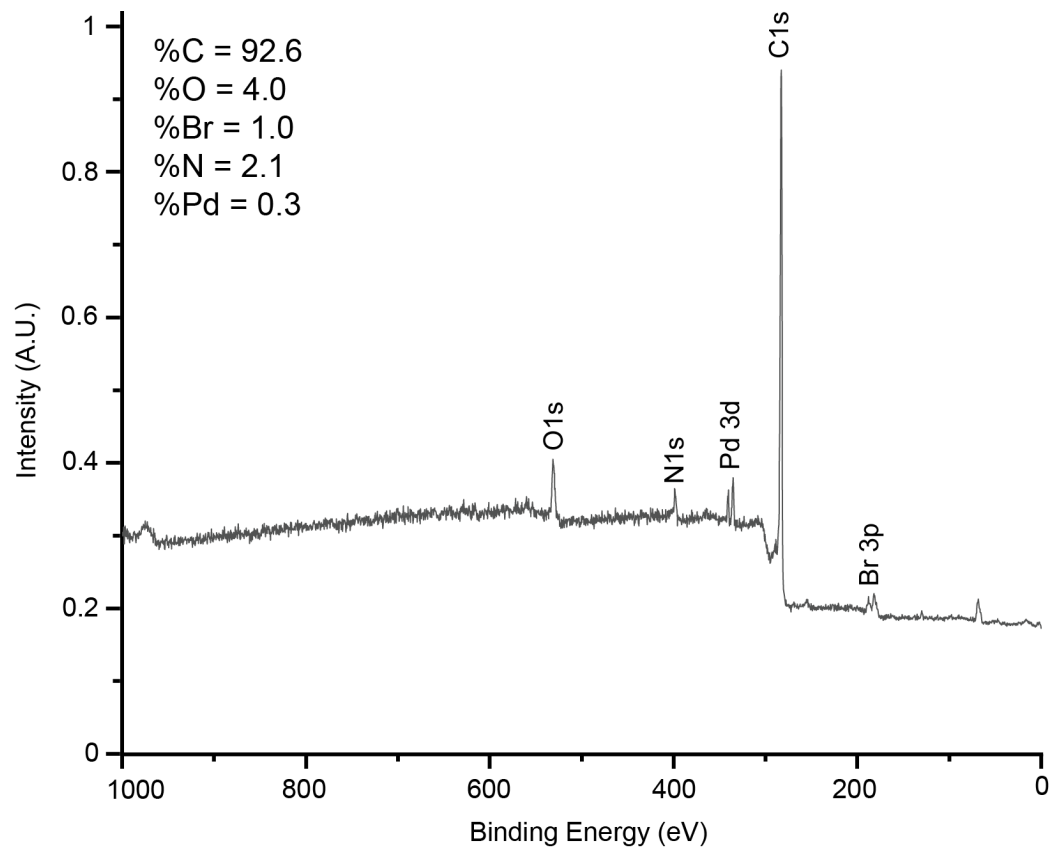


Figure S17. Survey XPS of **GY-Ph**.

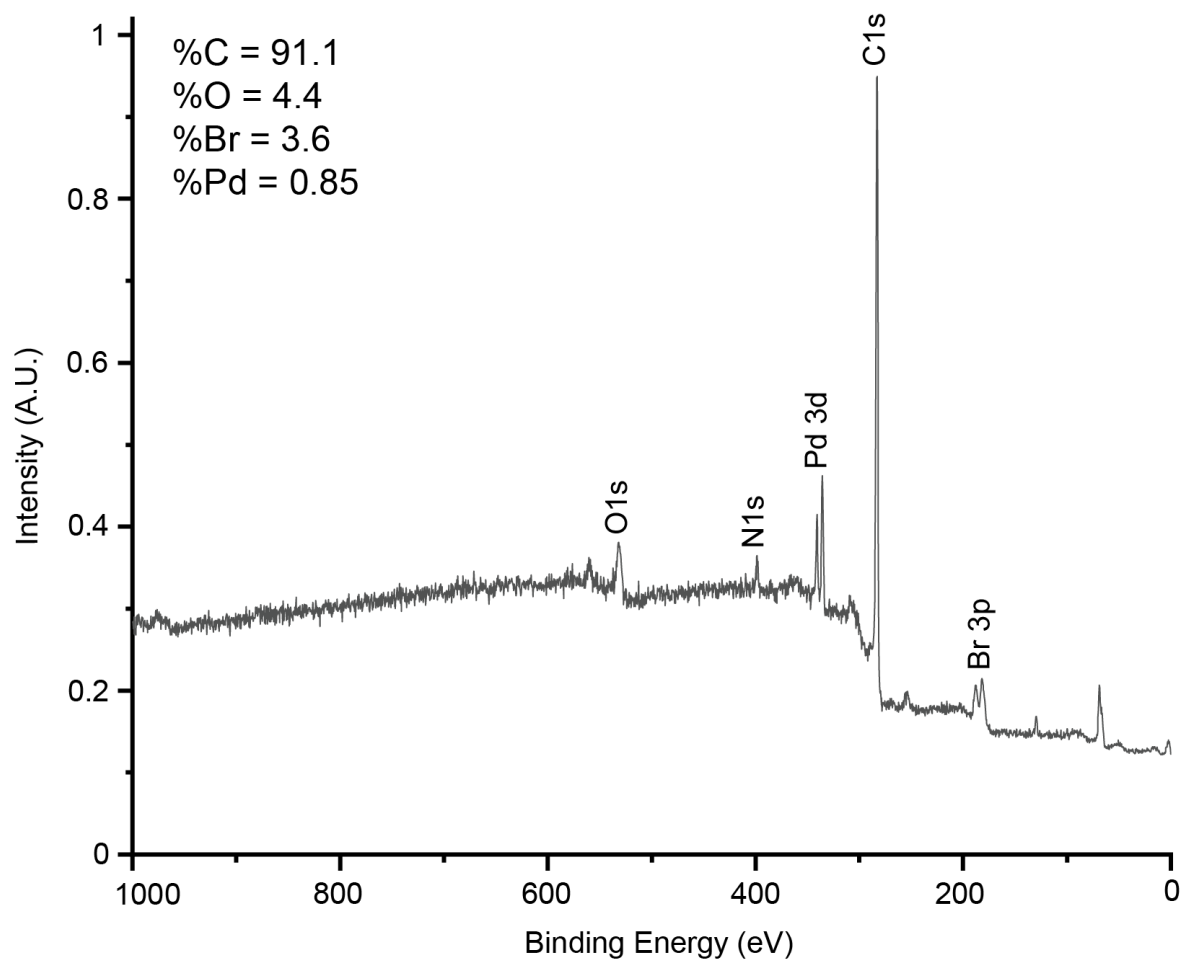


Figure S18. Survey XPS of GY-C₁₈.

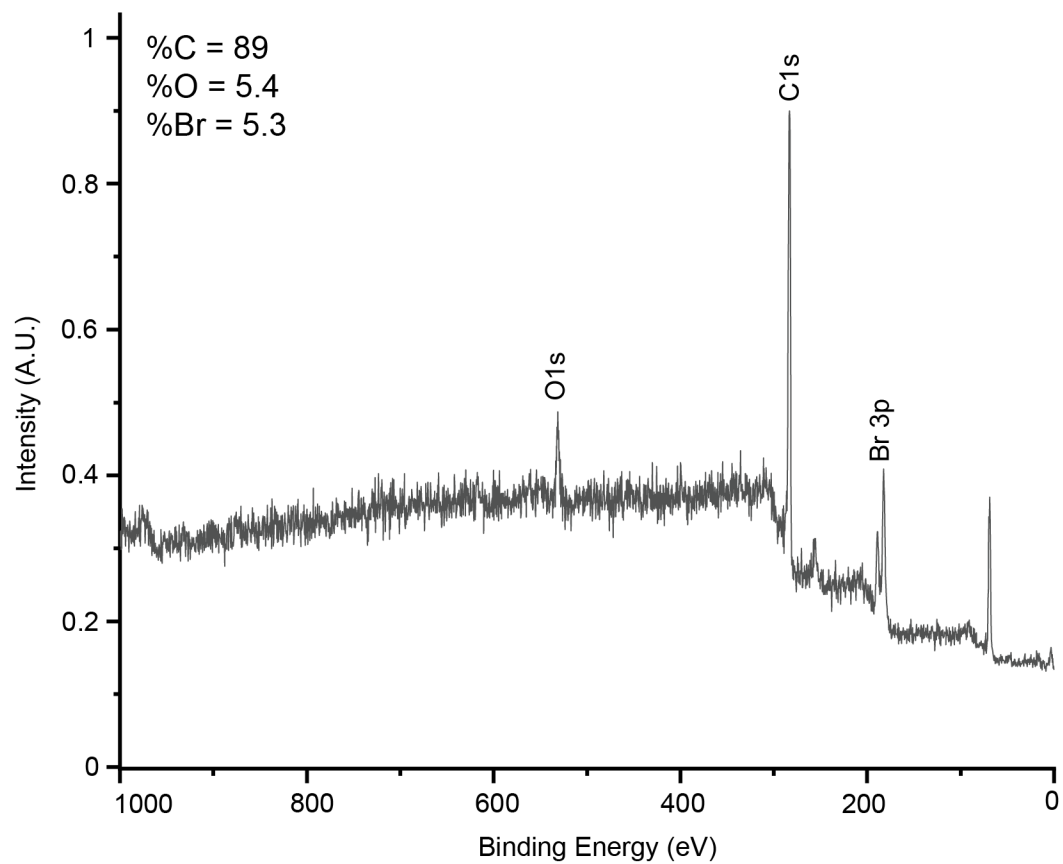


Figure S19. Survey XPS of GY-MeONaph.

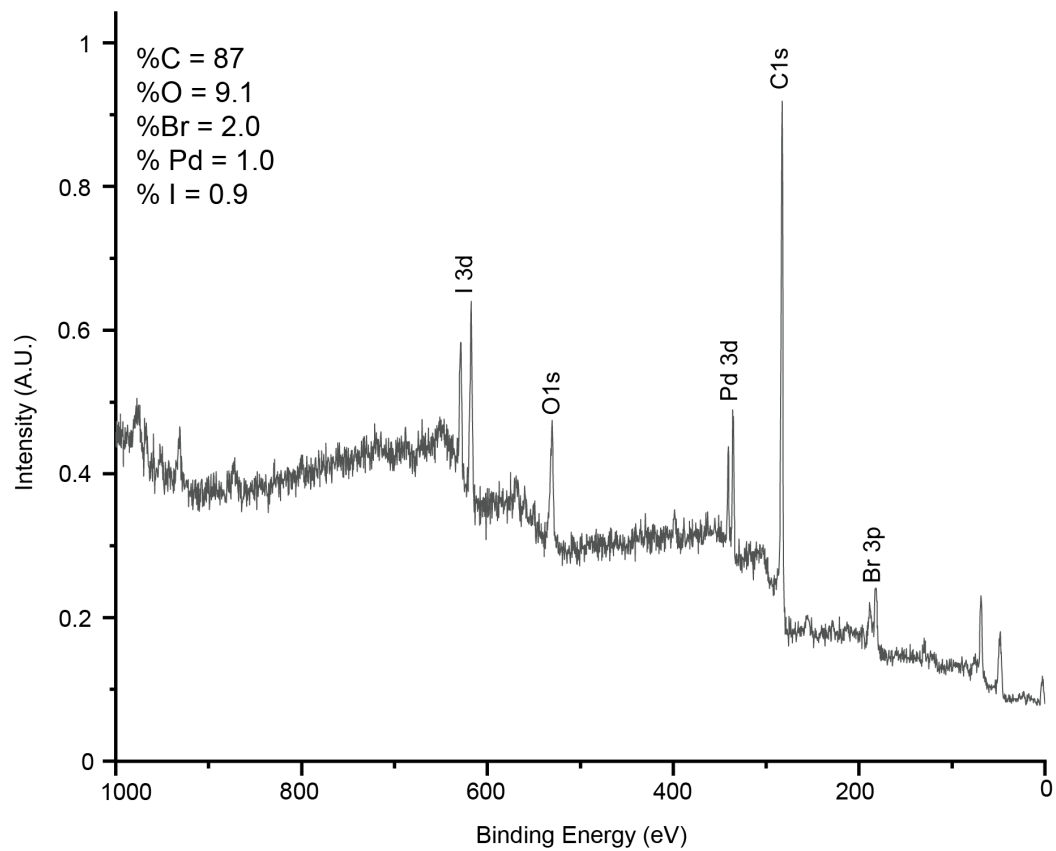


Figure S20. Survey XPS of GY-C₁₈N₃.

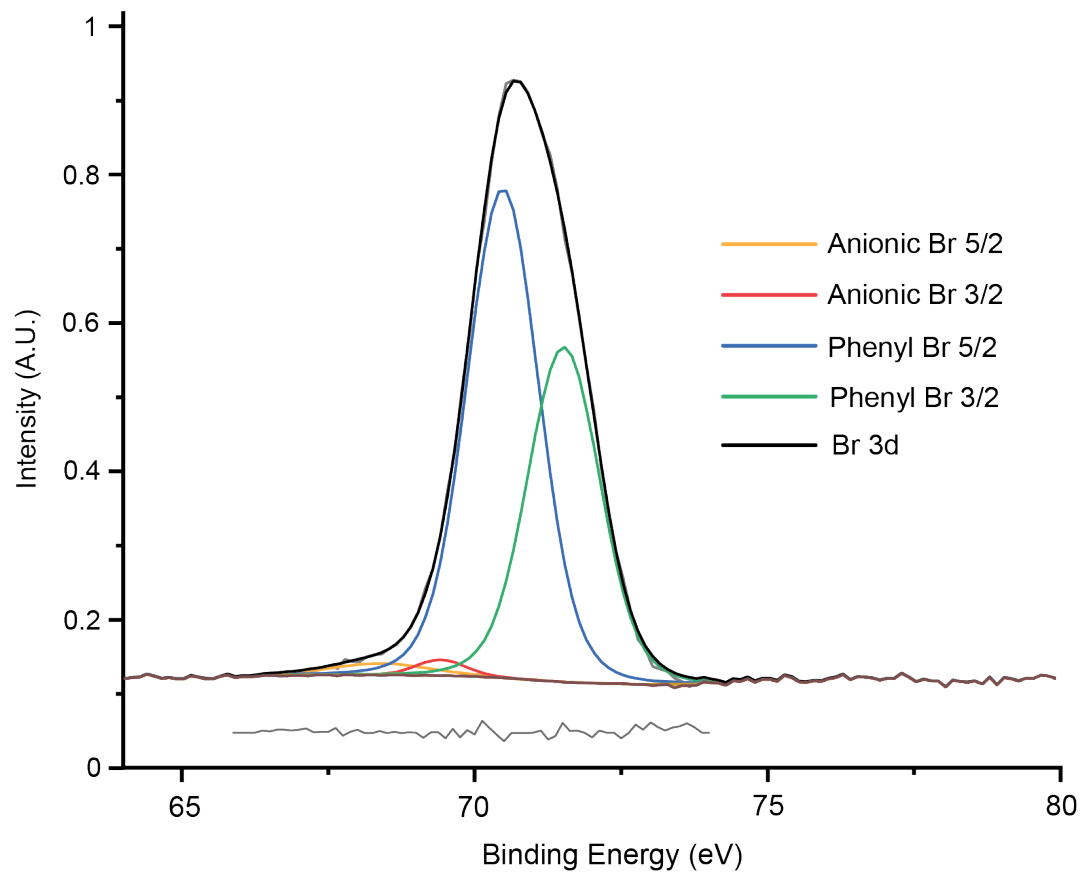


Figure S21. High-resolution Br 3d region XPS for **GY-Br** with fitting and residuals (gray).

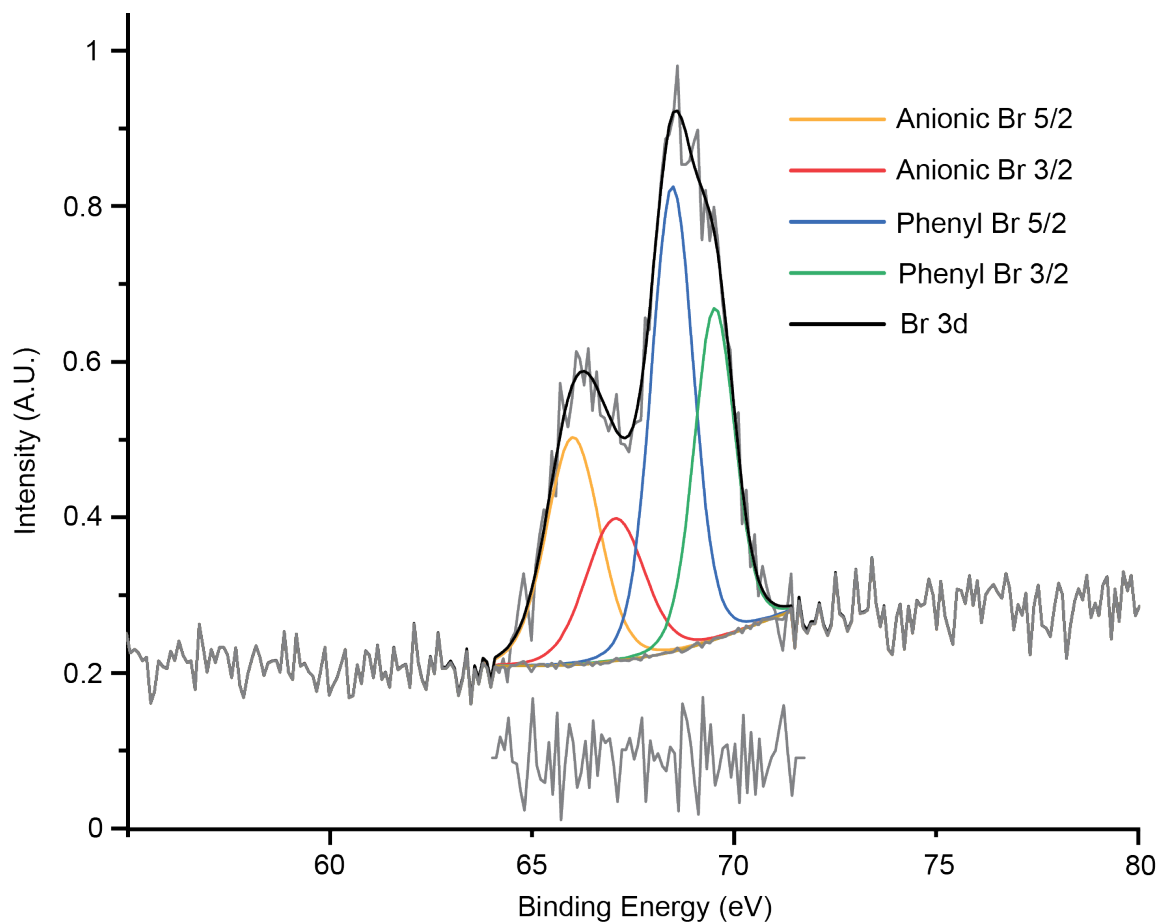


Figure S22. High-resolution Br 3d region XPS for **GY-Ph** with fitting and residuals (gray).

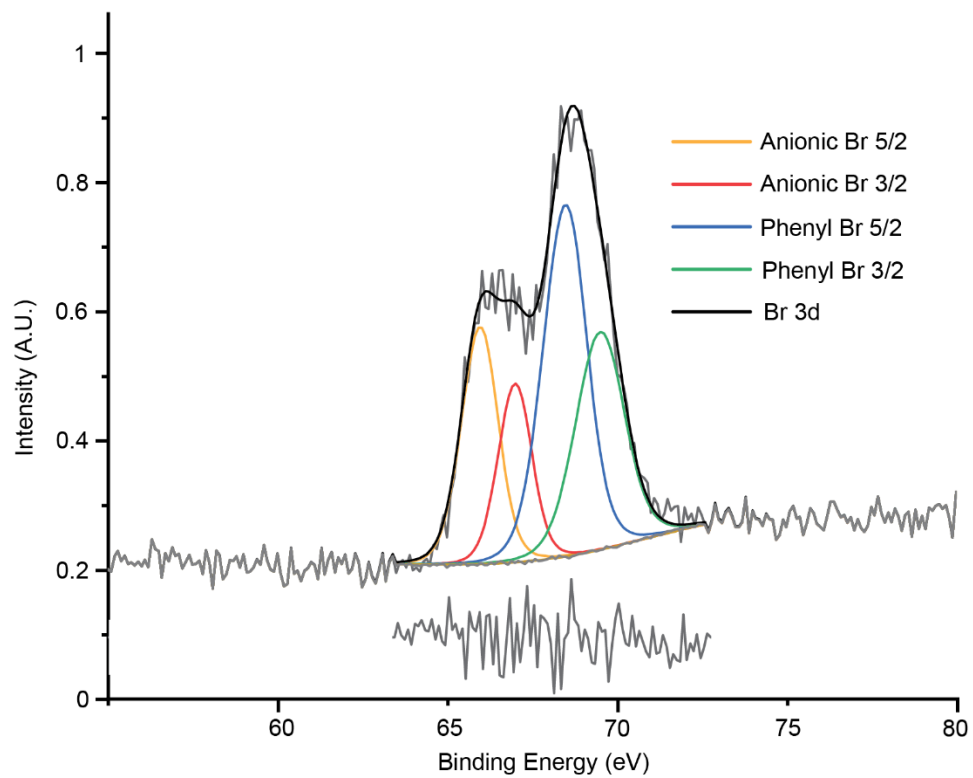


Figure S23. High-resolution Br 3d region XPS for GY-C₁₈ with fitting and residuals (gray).

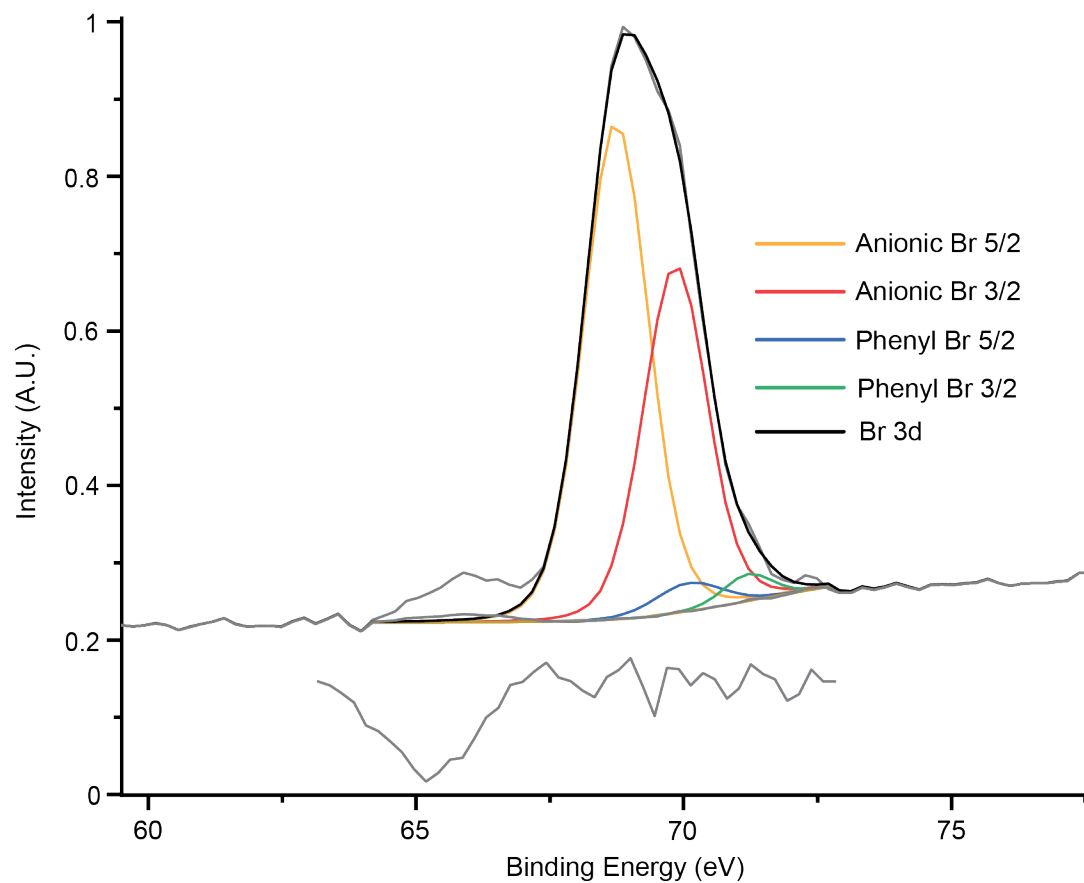


Figure S24. High-resolution Br 3d region XPS for **GY-MeONaph** with fitting and residuals (gray).

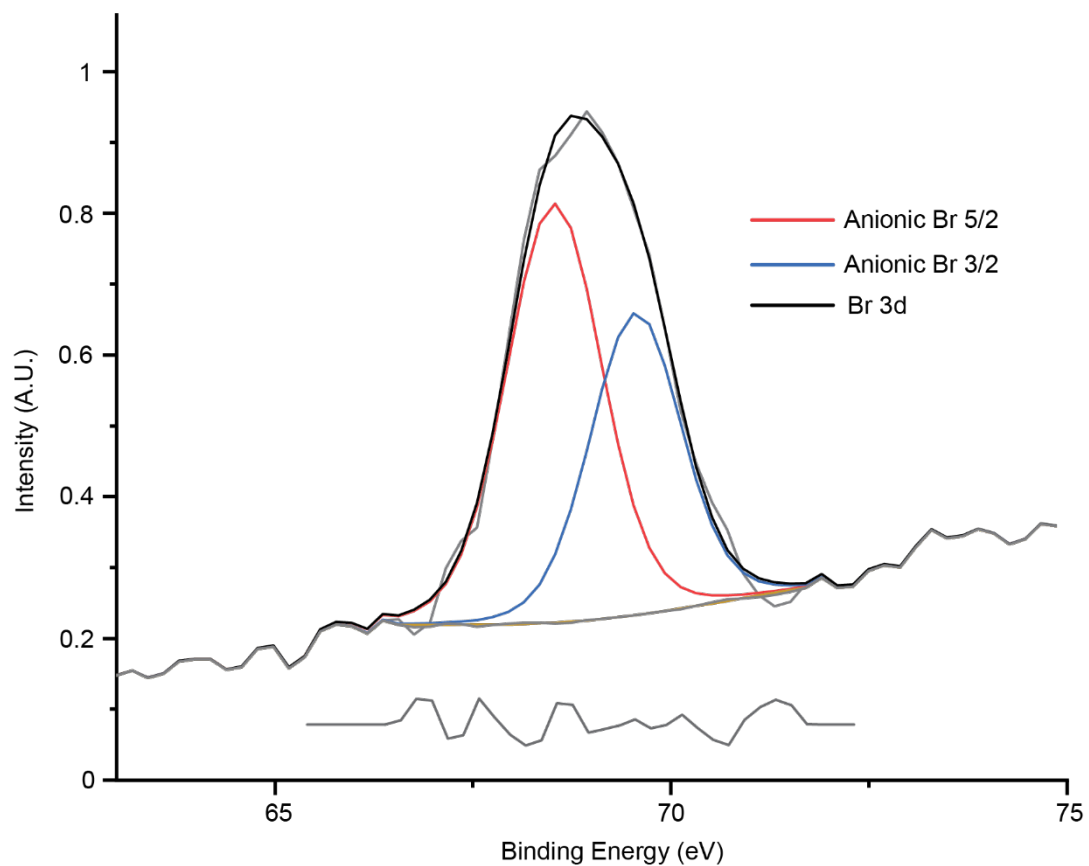


Figure S25. High-resolution Br 3d region XPS for GY-C₁₈N₃ with fitting and residuals (gray).

Material	N (at%)	Br (at%)	(Ar)C-Br (at%)	Pd (at%)
GY-Br	0.0	5.4	5.2	1.1
GY-Ph	2.1	1.0	0.6	0.3
GY-C₁₈	0.0	3.6	2.3	0.85
GY-MeO-Naph	0.3	5.3	0.3	0.0
GY-C₁₈N₃	0	2.0	0.0	1.0

Table S2. Nitrogen, bromine, and palladium content measured by XPS edge-functionalized γ -graphynes. Combined with survey, high-resolution Br 3d spectra were used to estimate the amount of edge-bound bromine.

TGA

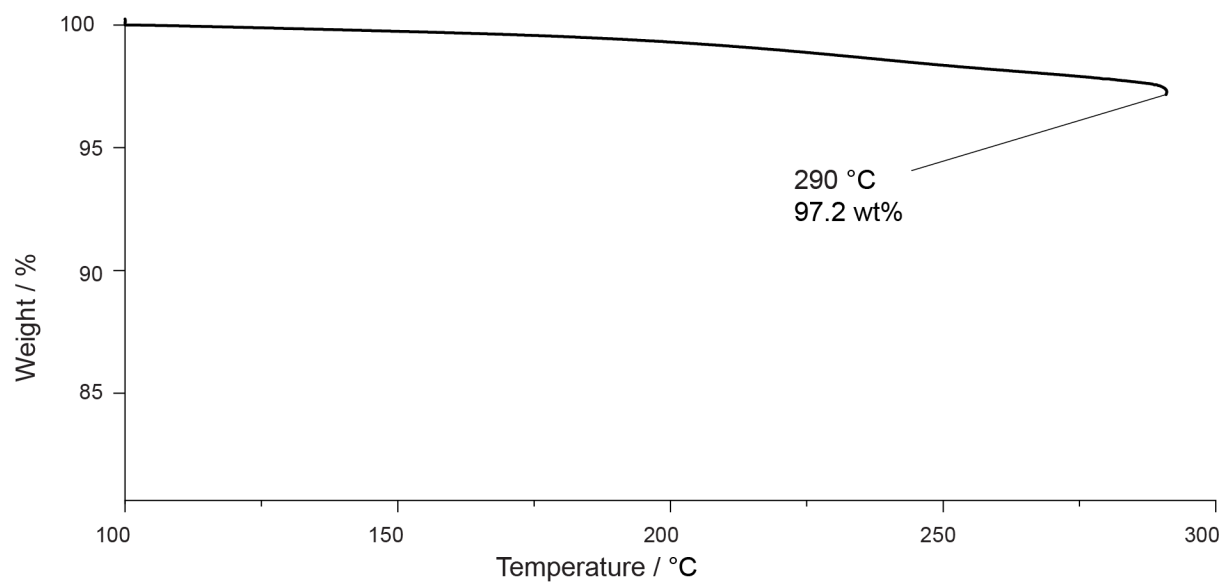


Figure S26. Thermogravimetric analysis of **GY-Br**.

TEM and SAED

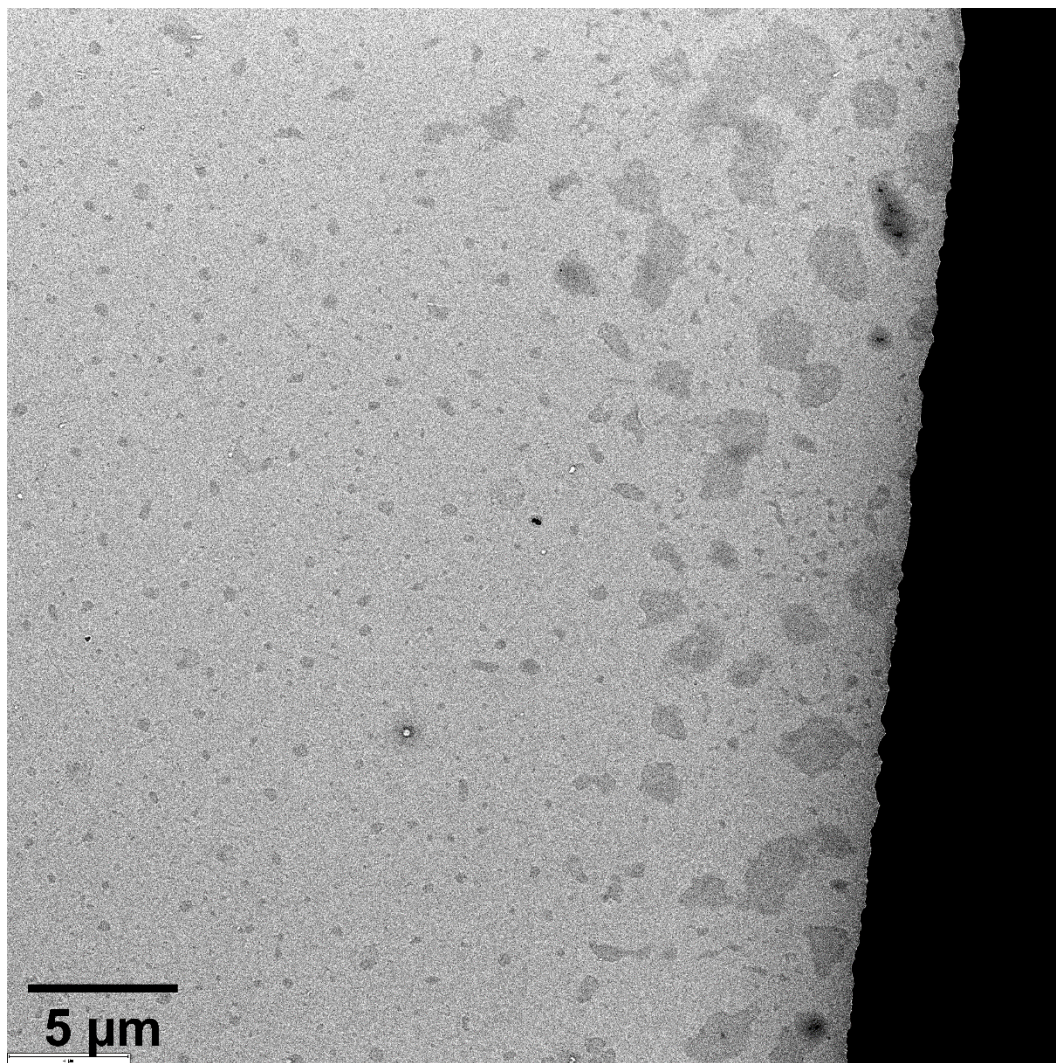


Figure S27. Representative bright-field TEM of **GY-Ph** with low-contrast thin flakes.

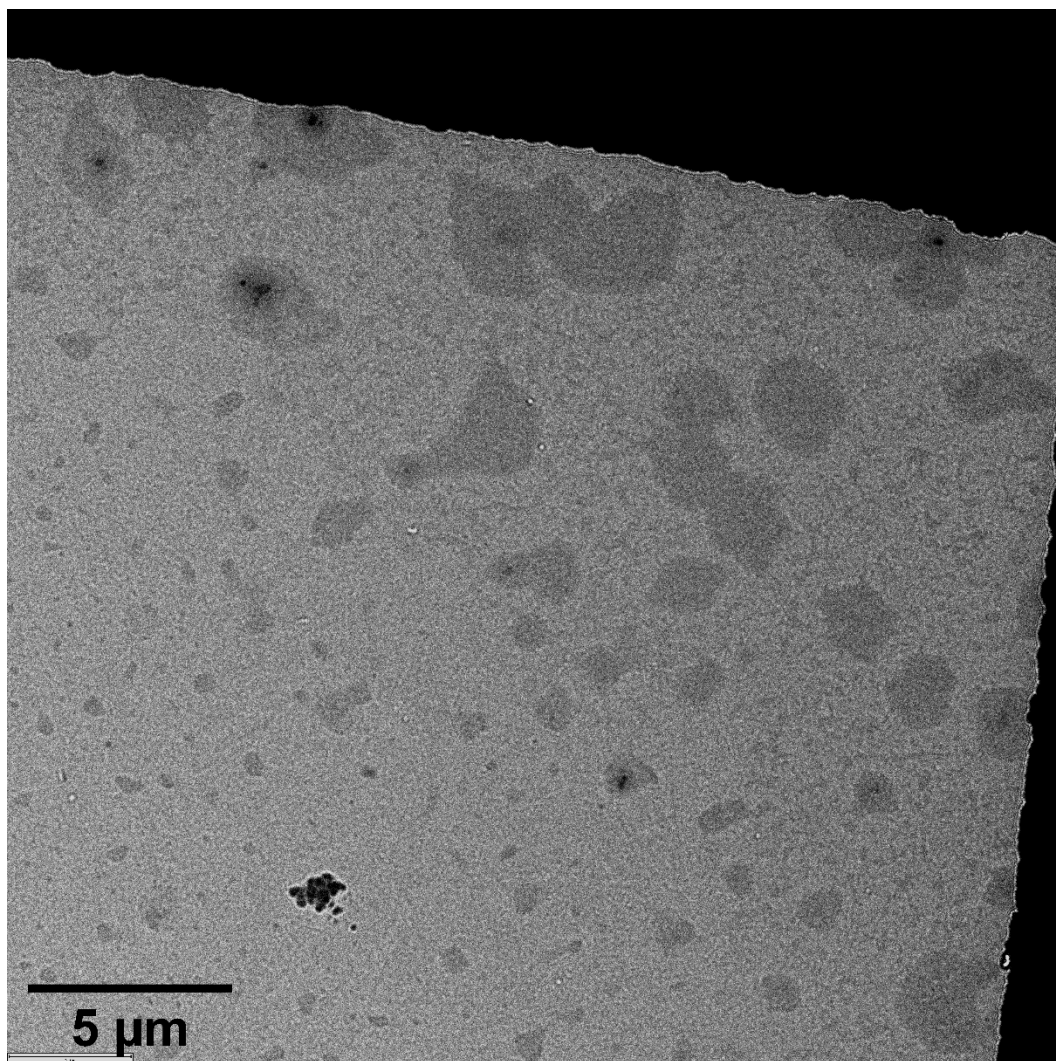


Figure S28. Representative bright-field TEM of **GY-Ph** with low-contrast thin flakes.

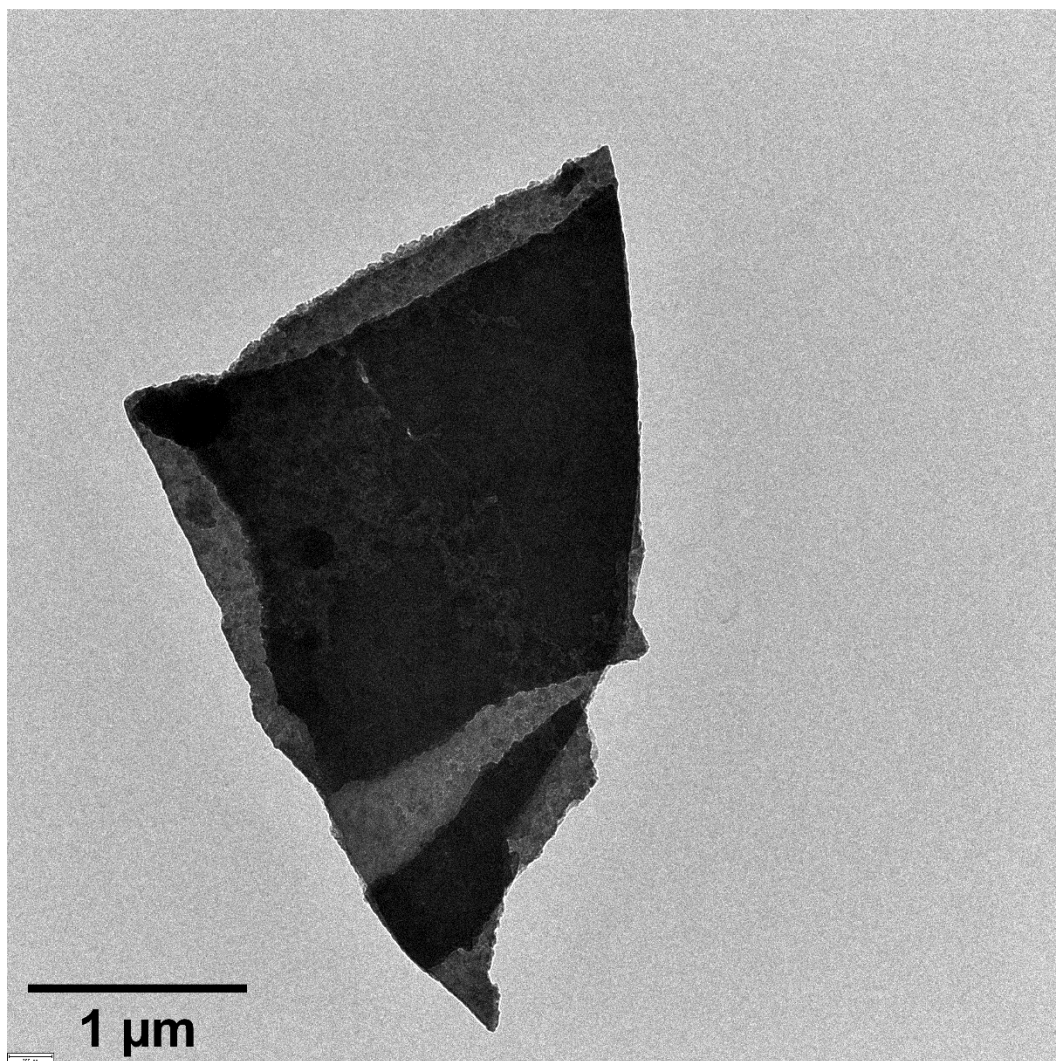


Figure S29. Bright-field TEM image of **GY-C18** displaying a layered/stepped structure.

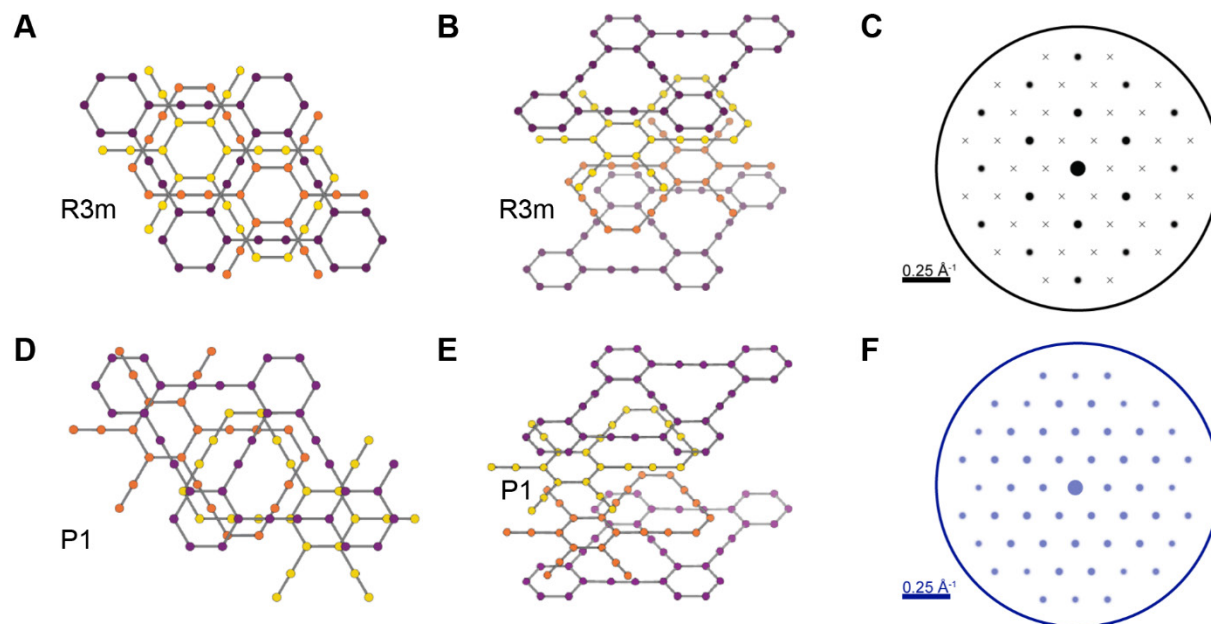


Figure S30. Impact of the stacking of γ -graphyne sheets on the basal plane SAED patterns. (A) Structural model of γ -graphyne stacked in the R3m space group, view in the c orientation. (B) View of the model in A rotated $\sim 45^\circ$ from the (0001) pole. (C) Simulated electron diffraction pattern for model in A in the c orientation. Systematic absences are represented by “x”. (D) Structural model of γ -graphyne stacked in the low-symmetry P1 space group, view in the c orientation. This is one of the infinite number of the possible stacking modes. (E) View of the model in D rotated $\sim 45^\circ$ from the (0001) pole. (F) Simulated electron diffraction pattern for model in D in the c orientation. This pattern features no systematic absences.

UV/Visible Spectroscopy of Dispersions

The dispersions shown in Fig. 2B were swirled gently and transferred via pipette to a glass cuvette with 10 mm path length. Sediment on the bottom of the vial was collected along with the solution. The cuvette was then rested for 2 minutes to allow the particles to settle. Then, each spectrum was collected against a reference cuvette of pure heptane. The absorbance at 600 nm was used to estimate optical density. This choice is arbitrary, as the absorbance of suspended graphyne is flat in the visible range between ~400-700 nm. The reason for lack of distinct spectral features is due to the length scale of graphyne particles, which is sufficient for the scattering of the incident light.

Material	GY-Br	GY-C₁₈N₃	GY-MeONaph	GY-C₁₈	GY-Ph
Absorbance (AU)	0.10	1.00	0.05	0.65	0.23

Table S3. OD₆₀₀ for each material suspended in heptane.

6. References

- (1) *CasaXPS*; Casa Software Ltd.: Teignmouth, United Kingdom, 2020.
- (2) Fairley, N.; Fernandez, V.; Richard-Plouet, M.; Guillot-Deudon, C.; Walton, J.; Smith, E.; Flahaut, D.; Greiner, M.; Biesinger, M.; Tougaard, S.; et al. Systematic and collaborative approach to problem solving using X-ray photoelectron spectroscopy. *Appl. Surf. Sci. Adv.* 2021, 5. DOI: 10.1016/j.apsadv.2021.100112.
- (3) Tougaard, S.; Jansson, C. Comparison of validity and consistency of methods for quantitative XPS peak analysis. *Surf. Interface Anal.* 1993, 20 (13), 1013-1046. DOI: 10.1002/sia.740201302 (accessed 2020-11-26 19:42:03).
- (4) Major, G. H.; Avval, T. G.; Patel, D. I.; Shah, D.; Roychowdhury, T.; Barlow, A. J.; Pigram, P. J.; Greiner, M.; Fernandez, V.; Herrera-Gomez, A.; et al. A discussion of approaches for fitting asymmetric signals in X-ray photoelectron spectroscopy (XPS), noting the importance of Voigt-like peak shapes. *Surf. Interface Anal.* 2021, 53 (8), 689-707. DOI: 10.1002/sia.6958.
- (5) Fairley, N. *CasaXPS Manual 2.3.15 Rev 1.2 : Introduction to XPS and AES*; Casa Software Ltd., 2009.
- (6) Beamson, G.; Briggs, D. *High Resolution XPS of Organic Polymers: The Scienta ESCA300 Database*; Wiley, 1992.
- (7) Steiner, U. B.; Caseri, W. R.; Suter, U. W.; Rehahn, M.; Schmitz, L. Ultrathin layers of low- and high-molecular-weight imides on gold and copper. *Langmuir* 1993, 9 (11), 3245-3254. DOI: 10.1021/la00035a079.
- (8) Loh, F. C.; Tan, K. L.; Kang, E. T. XPS studies of charge transfer interactions in some poly(N-vinylcarbazole)/acceptor complexes. *Eur. Polym. J.* 1991, 27 (10), 1055-1063. DOI: 10.1016/0014-3057(91)90079-4.
- (9) Klein, J. C.; Li, C. P.; Hercules, D. M.; Black, J. F. Decomposition of Copper Compounds in X-Ray Photoelectron Spectrometers. *Appl. Spectrosc.* 1984, 38 (5), 729-734.
- (10) Li, Y.; Chen, H.; Voo, L. Y.; Ji, J.; Zhang, G.; Zhang, G.; Zhang, F.; Fan, X. Synthesis of partially hydrogenated graphene and brominated graphene. *J. Mater. Chem.* 2012, 22 (30), 15021-15024. DOI: 10.1039/C2JM32307A.
- (11) Brant, P.; Stephenson, T. A. X-ray photoelectron spectra of mixed-valence diruthenium complexes. Distinguishing between strongly and weakly interacting metals in delocalized class III complexes. *Inorg. Chem.* 1987, 26 (1), 22-26. DOI: 10.1021/ic00248a006.
- (12) Nefedov, V.; Zakharova, I.; Moiseev, I.; Porai-Koshitz, M.; Vargaftik, M.; Belov, A. Study of palladium complex compounds by X-ray photoelectron spectroscopy. *Russ. J. Inorg. Chem.* 1973, 18 (12), 3264-3268.
- (13) Narita, N.; Nagai, S.; Suzuki, S.; Nakao, K. Optimized geometries and electronic structures of graphyne and its family. *Phys. Rev. B* 1998, 58 (16), 11009-11014. DOI: 10.1103/PhysRevB.58.11009.
- (14) Desyatkin, V. G.; Martin, W. B.; Aliev, A. E.; Chapman, N. E.; Fonseca, A. F.; Galvao, D. S.; Miller, E. R.; Stone, K. H.; Wang, Z.; Zakhidov, D.; et al. Scalable Synthesis and Characterization of Multilayer γ -Graphyne, New Carbon Crystals with a Small Direct Band Gap. *J. Am. Chem. Soc.* 2022, 144 (39), 17999-18008. DOI: 10.1021/jacs.2c06583.
- (15) *CrystalMaker*; CrystalMaker Software Ltd: Begbroke, Oxfordshire, England, 2020.
- (16) Momma, K.; Izumi, F. VESTA 3 for three-dimensional visualization of crystal, volumetric and morphology data. *J. Appl. Crystallogr.* 2011, 44 (6), 1272-1276. DOI: 10.1107/s0021889811038970.
- (17) Nielsen, K. T.; Bechgaard, K.; Krebs, F. C. Removal of Palladium Nanoparticles from Polymer Materials. *Macromolecules* 2005, 38 (3), 658-659. DOI: 10.1021/ma047635t.
- (18) Johnson, N. A.; Wolfe, S. R.; Kabir, H.; Andrade, G. A.; Yap, G. P. A.; Heiden, Z. M.; Moberly, J. G.; Roll, M. F.; Waynant, K. V. Deconvoluting the Innocent vs. Non-Innocent Behavior of N,N-Diethylphenylazothioformamide Ligands with Copper Sources. *Eur. J. Inorg. Chem.* 2017, 2017 (47), 5576-5581. DOI: 10.1002/ejic.201701097.